IDENTIFICATION OF STRUCTURAL CHANGES ASSOCIATED WITH REGULATION OF TYROSINE HYDROXYLASE

A Dissertation

by

SHANZHI WANG

Submitted to the Office of Graduate Studies of
Texas A&M University
in partial fulfillment of the requirements for the degree of

DOCTOR OF PHILOSOPHY

August 2010

Major Subject: Biochemistry

IDENTIFICATION OF STRUCTURAL CHANGES ASSOCIATED WITH REGULATION OF TYROSINE HYDROXYLASE

A Dissertation

by

SHANZHI WANG

Submitted to the Office of Graduate Studies of
Texas A&M University
in partial fulfillment of the requirements for the degree of

DOCTOR OF PHILOSOPHY

Approved by:

Co-Chairs of Committee,	Paul F. Fitzpatrick
	Gregory D. Reinhart
Committee Members,	Michael Polymenis
	David P. Barondeau
Head of Department,	Gregory D. Reinhart

August 2010

Major Subject: Biochemistry

ABSTRACT

Identification of Structural Changes Associated with Regulation of Tyrosine Hydroxylase. (August 2010)

Shanzhi Wang, B.S., Jilin University

Co-Chairs of Advisory Committee: Dr. Paul F. Fitzpatrick
Dr. Gregory D. Reinhart

Tyrosine hydroxylase (TyrH) is the first and rate-limiting enzyme of catecholamine synthetic pathway, and its regulation is critical for controlling catecholamine synthesis. The well recognized regulatory mechanisms are inhibition by catecholamine binding and re-activation upon Ser40 phosphorylation. Catecholamines bind to TyrH tightly, while phosphorylation of TyrH at Ser40 decreases the binding affinity by several hundred-fold. Regulation of TyrH is accompanied by conformational changes of the protein. This study focuses on the identification of the conformational changes of TyrH upon dopamine binding and Ser40 phosphorylation, using hydrogen deuterium exchange mass spectrometry (HDMS) and fluorescence spectroscopy.

HDMS identifies three peptides undergoing conformational changes upon dopamine binding, peptide 35-41, 42-71 and 295-299. Peptides 35-41 and 42-71 are on the regulatory domain, while peptide 295-299 is at the active site entrance. Upon dopamine binding, all three peptides are protected from exchange; phosphorylation of TyrH at Ser40 has opposite effects on the exchange kinetics of peptide 295-299, but peptides 35-41 and 42-71 could not be detected by MS after phosphorylation. This

suggests that the structural effects of dopamine binding and Ser40 phosphorylation are opposite.

The fluorescence spectroscopy of mutant enzymes containing a single tryptophan at position 14, 34 or 74 was performed before and after phosphorylation. F34W/F_3W TyrH has a significant decrease in steady-state fluorescence anisotropy, an increase in the bimolecular quenching rate constant k_q and dynamic anisotropy upon phosphorylation at Ser40, while F14W/F_3W TyrH and F74W/F_3W TyrH exhibit much smaller differences. This suggests that phosphorylation of TyrH at Ser40 increases the flexibility of the regulatory domain.

The results are consistent with TyrH existing in two conformations, a closed conformation stabilized by dopamine in which the N-terminal regulator domain of TyrH covers the active site entrance and an open conformation stabilized by phosphorylation in which the regulatory domain has moved away from the active site entrance.

DEDICATION

This dissertation is dedicated to my family: to my parents, who give me unconditional love and teach me to how to work, to love and to believe; to my wife, the most determined person I ever saw, who makes me a better person and makes my life whole; to my daughter, who is a blessing to my family and also brings all the joy and responsibility.

ACKNOWLEDGEMENTS

I am very grateful to my adviser Dr. Paul F. Fitzpatrick, who has been a very patient and knowledgeable advisor. I am honored to be working with him. I thank my collaborators Dr. Reinhart and Mauricio, who have been friendly, generous and supportive. I thank my committee members for their overseeing my progress during my Ph.D. study. I thank all of my lab peers, with whom it has been enjoyable to work and share. I made many friends in graduate school and their friendship is greatly appreciated. I am in debt to my family, who gives me tremendous support and love during the difficult times and makes the good times meaningful.

ABBREVIATIONS

TyrH	Tyrosine hydroxylase
DOPA	Dihydroxyphenylalanine
PheH	Phenylalanine hydroxylase
TrpH	Tryptophan hydroxylase
BH_4	Tetrahydrobiopterin
PKA	Protein kinase A
ACT	Aspartate kinase – chorismate mutase – TyrA
CvPheH	PheH from Chromobacterium violaceum
K_{SV}	Stern-Volmer quenching constant

TABLE OF CONTENTS

Page

ABSTRACT iii

DEDICATION v

ACKNOWLEDGEMENTS vi

ABBREVIATIONS vii

TABLE OF CONTENTS viii

LIST OF FIGURES x

LIST OF TABLES xii

CHAPTER

I INTRODUCTION 1

Catecholamine Synthetic Pathway 1
Aromatic Amino Acid Hydroxylase Family 3
Structures of the Aromatic Amino Acid Hydroxylases 6
Mechanism 13
Regulation 18

II IDENTIFICATION OF STRUCTURAL CHANGES ASSOCIATED WITH REGULATION OF TYROSINE HYDROXYLASE BY HYDROGEN/DEUTERIUM EXCHANGE MASS SPECTROMETRY 25

Experimental Procedures 27
Results 31
Discussion 37

CHAPTER Page

III FLUORESCENCE ANISOTROPY REVEALS EFFECTS OF SER40 PHOSPHORYLATION ON THE DYNAMICS OF A REGION IN THE REGULATORY DOMAIN OF TYROSINE HYDROXYLASE 44

Experimental Procedures 47
Results 49
Discussion 57

IV IDENTIFICATION OF A DIMERIZATION DOMAIN WITHIN THE REGULATORY DOMAIN OF TYROSINE HYDROXYLASE 64

Experimental Procedures 66
Results 68
Discussion 79

V SUMMARY 84

REFERENCES 87

VITA 107

LIST OF FIGURES

FIGURE		Page
1.1	Catecholamine biosynthetic pathway	2
1.2	The reactions catalyzed by aromatic amino acid hydroxylases	4
1.3	Sequence alignment of rat TyrH, PheH and TrpH	5
1.4	Structures of the catalytic domains of TyrH, PheH and TrpH	7
1.5	The re-constructed structure of PheH	8
1.6	BH_4 and amino acid binding sites of PheH	10
1.7	Proposed chemical mechanism of TyrH	13
1.8	Regulatory mechanism of TyrH	20
1.9	Regulatory mechanism of PheH	22
2.1	Peptic peptides of TyrH used in the hydrogen deuterium exchange mass spectrometry experiments	31
2.2	The extent of deuterium incorporation into peptides in the catalytic domain of TyrH at various times	33
2.3	Time course of deuterium incorporation into peptides 28-34, 266-273, 349-354 and 467-487 for TyrH alone	34
2.4	Time course of deuterium incorporation into peptides 35-41, 42-72, and 295-299 for TyrH alone, with bound dopamine or phosphorylated at Ser40	36
2.5	Sequence alignment of TyrH and PheH regulatory domains	40
2.6	Interactions between the regulatory and catalytic domains of PheH	41

FIGURE Page

3.1 Regulation of TyrH 45

3.2 Fluorescence quenching by acrylamide of F14W/F_3W TyrH, F34W/F_3W TyrH and F74W/F_3W TyrH..... 51

3.3 Dynamic anisotropy of F14W/F_3W TyrH, F34W/F_3W TyrH and F74W/F_3W TyrH 56

3.4 Interaction between the regulatory domain and the catalytic domain of PheH..... 61

4.1 Deuterium incorporation into peptide 342-348 of wild-type TyrH and Δ155 TyrH in the absence and presence of 400 μM tyrosine..... 69

4.2 HDMS spectra of residues 488-498 of Δ155 TyrH in the absence and presence of 400 μM tyrosine. 70

4.3 Deuterium incorporation into the tetramerization domain of Δ155 TyrH in the absence and presence of 400 μM tyrosine..... 71

4.4 Effects of tyrosine binding on the quaternary structure of Δ155 TyrH 74

4.5 Analysis of the influence of phenylalanine on quaternary structure of wild-type TyrH 75

4.6 Analysis of the quaternary structure of 54k TyrH by gel-filtration..... 76

4.7 Analysis of the influence of phenylalanine on quaternary structures of Δ32 TyrH and Δ68 TyrH by gel-filtration..... 78

4.8 The structure of PheH 81

LIST OF TABLES

TABLE Page

3.1 Steady-state parameters and dopamine dissociation rate constants of F14W/F3W TyrH, F34W/F3W TyrH and F74W/F3W TyrH 50

3.2 Effects of phosphorylation on the fluorescence parameters of F14W/F_3W TyrH, F34W/F_3W TyrH and F74W/F_3W TyrH 52

CHAPTER I

INTRODUCTION

CATECHOLAMINE SYTHETIC PATHWAY

Catecholamines are neurotransmitters released from the sympathetic nervous system. They are also called “fight and flight” hormones, because they are largely released in response to stress. The name catecholamine comes from the common chemical composition, a catechol group and an amine group. Because they serve as neurotransmitters, the disturbance of their homeostasis can lead to disease. The overproduction of catecholamines can result in hypertension (*1*) due to their sympathetic stimulation, while decreased production of them, especially dopamine, can cause central nervous system problems, e.g., Parkinson’s disease (*2*) and DOPA-responsive dystonia (Segawa’s disease) (*3*). Dopamine, nonepinephrine and epinephrine are the most abundant catecholamines; others are synthesized using them as backbones.

As shown in Figure 1.1, the synthesis of catecholamines starts from tyrosine. In this step, tyrosine hydroxylase (TyrH) catalyzes the hydroxylation of the aromatic ring of tyrosine to form dihydroxyphenylalanine (DOPA), using molecular oxygen and tetrahydrobiopterin (*4, 5*). This step is the rate-limiting step in the catecholamine synthetic pathway and is subject to regulation (*4*). The following step is decarboxylation of DOPA to form dopamine; this step is catalyzed by the enzyme DOPA decarboxylase using cofactor pyridoxal phosphate (*6*). Next, the production of nonepinephrine is

---

This dissertation follows the style of *Biochemistry*.

catalyzed by the enzyme dopamine β-hydroxylase using molecular oxygen and ascorbic acid (*6*). Finally, the enzyme phenylethanolamine *N*-methyltransferase catalyzes the conversion of norepinephrine into epinephrine, using S-adenosyl-methionine (*6*).

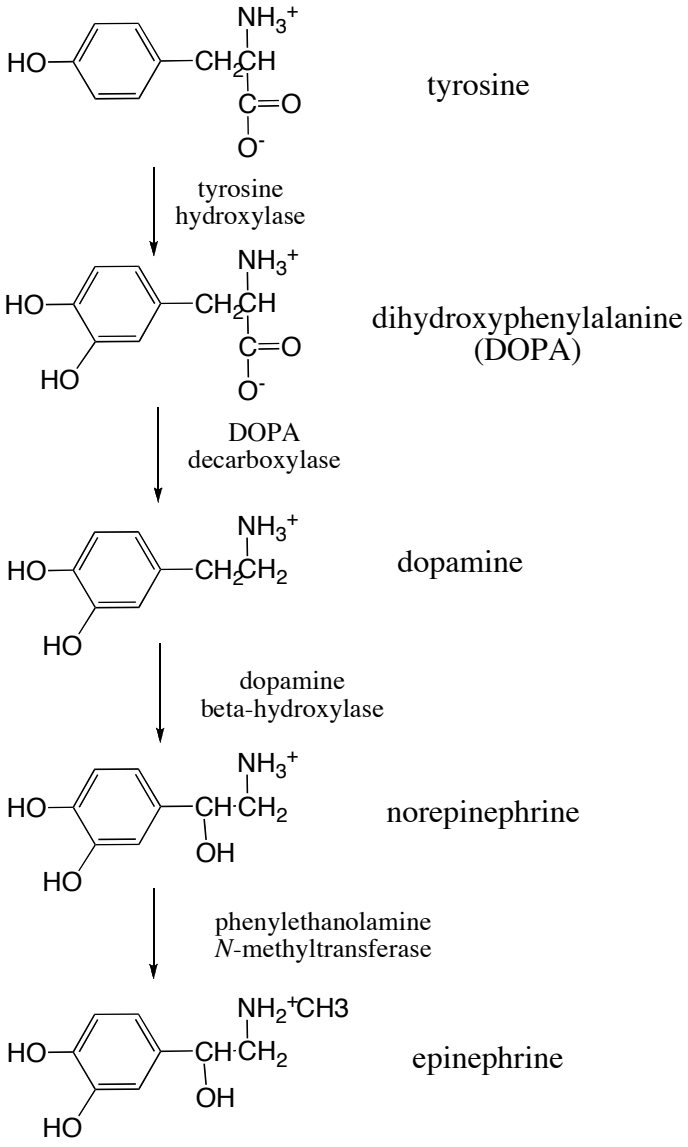

Figure 1.1: Catecholamine biosynthetic pathway.

Catecholamines can be degraded either by catechol-*O*-methyltransferases (COMT) (*7*) or by monoamine oxidases (MAO) (*8*). COMT transfers a methyl group to one of the hydroxyl groups on the catechol, while MAO oxidizes the amine group to form an aldehyde group.

AROMATIC AMINO ACID HYDROXYLASE FAMILY

TyrH is found in the central nervous system and adrenal medulla. It belongs to the small family of aromatic amino acid hydroxylases, which also includes phenylalanine hydroxylase (PheH) and tryptophan hydroxylase (TrpH). PheH is a liver enzyme that catalyzes the catabolism of excess phenylalanine into tyrosine, the first step of phenylalanine degradation. A deficiency of this enzyme can lead to phenylalanine accumulation in the body and contributes to most of the cases of phenylketonuria (*9*). TrpH is found in the gastrointestinal tract and central nervous systems. It catalyzes the first step in the biosynthesis of serotonin, the formation of 5-hydroxytryptophan from tryptophan (*10*); a deficiency of this enzyme can lead to depression (*11*). As shown in Figure 1.2, the hydroxylation of all three aromatic amino acids requires molecular oxygen and tetrahydrobiopterin. In addition, a non-heme ferrous iron is required at the active site for catalysis (*12-14*). All three enzymes are composed of an N-terminal regulatory domain, a catalytic domain and a tetramerization domain at the very C-terminus(*15-20*). The rat forms of the enzymes share a sequence identity of ~50% in the catalytic domains, but less than 15% sequence identity in the regulatory domains (Figure 1.3). It is generally accepted that they share a common chemical mechanism (*21*), but have distinct regulatory mechanisms (*5*).

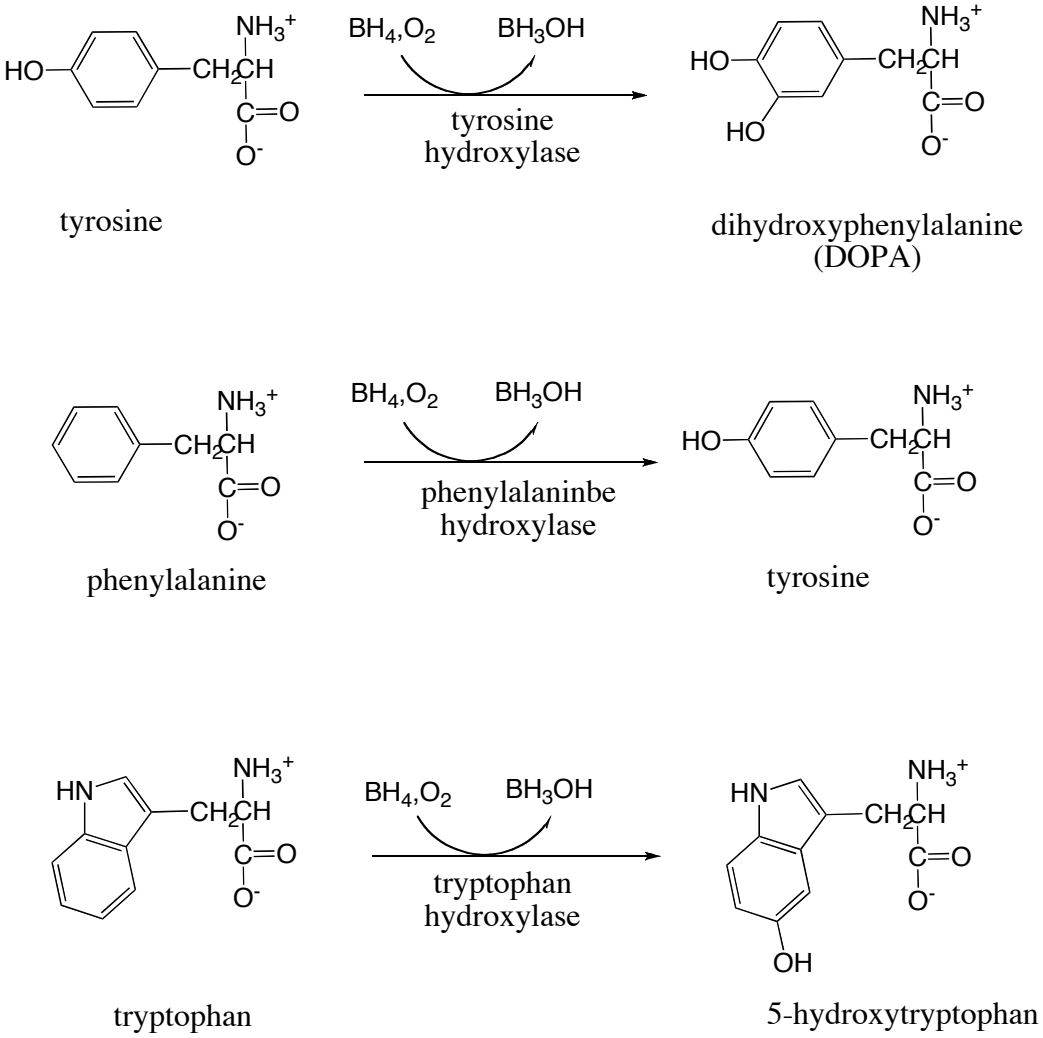

Figure 1.2: The reactions catalyzed by aromatic amino acid hydroxylases.

```
TyrH  MPTPSAPSPQPKGFRRAVSEQDAKQAEAVTSPRFIGRRQSLIEDARKEREAAAAAAAAAV 60
PheH  --------------MAAVVLENGVLSRKLSD---FGQETSYIEDNSNQN----------- 32
TrpH  ------------------MIED-------------NKEN---KDHSSER----------- 15
                                              *

TyrH  ASSEPGNPLEAVVFEERDGNAVLNLLFSLRGTKPSSLSRAVKVFETFEAKIHHLETRPAQ 120
PheH  --------------------GAISLIFSLK-EEVGALAKVLRLFEENDINLTHIESRPSR 71
TrpH  --------------------GRVTLIFSLK-NEVGGLIKALKIFQENHVNLLHIESRKSK 54
                             * ***       *      *        * * *
                                                          ▼
TyrH  RPLAGSPHLEYFVRFEVPSGDLAALLSSVRRVSDDVRSARED----------KVPWFPRK 170
PheH  L---NKDEYEFFTYLDKRSKPV--LGSIIKSLRNDIGATVHELSRDKE--KNTVPWFPRT 124
TrpH  R---RNSEFEIFVDCDINREQLNDIFPLLKSHTTVLSVDSPDQLPEKEDVMETVPWFPKK 111
               * *                                            *****

TyrH  VSELDKCHHLVTKFDPDLDLDHPGFSDQVYRQRRKLIAEIAFQYKHGEPIPHVEYTAEEI 230
PheH  IQELDRFANQILSYGAELDADHPGFKDPVYRARRKQFADIAYNYRHGQPIPRVEYTEEEK 184
TrpH  ISDLDFCANRVLLYGSELDADHPGFKDNVYRRRRKYFAELAMNYKHGDPIPKIEFTEEEI 171
         **            ** ***** * *** ***  *  *  * ** ***  * * **

TyrH  ATWKEVYVTLKGLYATHACREHLEGFQLLERYCGYREDSIPQLEDVSRFLKERTGFQLRP 290
PheH  QTWGTVFRTLKALYKTHACYEHNHIFPLLEKYCGFREDNIPQLEDVSQFLQTCTGFRLRP 244
TrpH  KTWGTIFRELNKLYPTHACREYLRNLPLLSKYCGYREDNVPQLEDVSNFLKERTGFSIRP 231
       **      *  ** **** *      **  *** ***  ******* **   ***  **

TyrH  VAGLLSARDFLASLAFRVFQCTQYIRHASSPMHSPEPDCCHELLGHVPMLADRTFAQFSQ 350
PheH  VAGLLSSRDFLGGLAFRVFHCTQYIRHGSKPMYTPEPDICHELLGHVPLFSDRSFAQFSQ 304
TrpH  VAGYLSPRDFLSGLAFRVFHCTQYVRHSSDPLYTPEPDTCHELLGHVPLLAEPSFAQFSQ 291
      *** ** ****  ****** **** ** * *   **** *********      ******

TyrH  DIGLASLGASDEEIEKLSTVYWFTVEFGLCKQNGELKAYGAGLLSSYGELLHSLSEEPEV 410
PheH  EIGLASLGAPDEYIEKLATIYWFTVEFGLCKEGDSIKAYGAGLLSSFGELQYCLSDKPKL 364
TrpH  EIGLASLGASEETVQKLATCYFFTVEFGLCKQDGQLRVFGAGLLSSISELRHALSGHAKV 351
       ********  *   ** * * *********        *******  **   **

TyrH  RAFDPDTAAVQPYQDQTYQPVYFVSESFNDAKDKLRNYASRIQRPFSVKFDPYTLAIDVL 470
PheH  LPLELEKIACQEYSVTEFQPLYYVAESFSDAKEKVRTFAATIPRPFSVRYDPYTQRVEVL 424
TrpH  KPFDPKVACKQECLITSFQDVYFVSESFEDAKEKMREFAKTVKRPFGVKYNPYTQSIQVL 411
               *       *  * * *** *** * *  *    *** *   ***    **

TyrH  DSPHTIQRSLEGVQDELHTLAHALSAIS----- 498
PheH  DNTQQLKILADSINSEVGILCNALQKIK----- 452
TrpH  RDSKSITSAMNELRHDLDVVNDALARVSRWPSV 444
                           **
```

Figure 1.3: Sequence alignment of rat TyrH, PheH and TrpH. The default parameters of Clustal W2 were used. Conserved residues are indicated using *, and the start of the catalytic domain is indicated by a solid triangle.

STRUCTURES OF THE AROMATIC AMINO ACID HYDROXYLASES

There are several structures available for various forms of the three enzymes, with most structures of PheH. As expected, the catalytic domains have very high structurally similarity (Figure 1.4). The active site is a 10 Å deep and 17 Å wide cleft containing a non-heme iron atom chelated by two conserved histidines and one conserved glutamate (*13, 14, 22*). In rat TyrH, His331 and His336 were identified as iron-chelating residues by mutagenesis studies before the crystal structure became available (*23*), while the corresponding residues in rat PheH, His285 and His290, were also identified prior to the crystal structure (*24*). Although the third iron-chelating residue was not directly identified by mutagenesis studies, its presence as a carboxylic amino acid had been predicted (*21*). This facial triad motif is used by a variety of non-heme iron binding enzymes (*25*); unlike other enzymes with the same motif, the substrates of the three aromatic amino acid hydroxylases do not directly coordinate to the iron. The C-terminal 45 residues contain a long α-helix at the very end and two short β-sheets. The β-sheets of two adjacent subunits form hydrogen bonds, while the α-helices of four subunits form a coiled-coil tetramer (*13, 14*). The coiled-coil structure had been predicted based on its sequence and mutagenesis studies (*26, 27*). Mutations of the coiled-coil of TyrH dissociate the tetramer into dimers (*27*), while additional deletion of the N-terminal regulatory domain yields monomers (*26*).

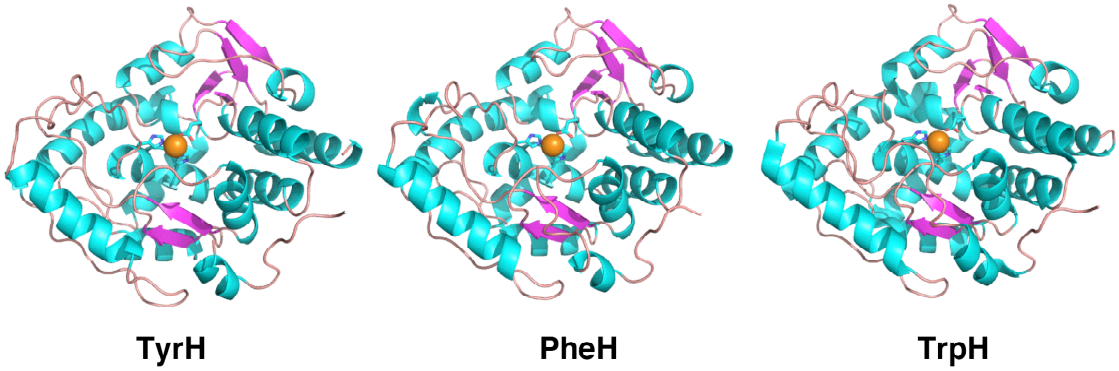

Figure 1.4: Structures of the catalytic domains of TyrH (1TOH), PheH (2PHM) and TrpH (1MLW).

A structure of the regulatory domain is only available for PheH, although the first eighteen residues are missing from the structure (*28*). The protein is a dimer due to the deletion of the C-terminal 25 residues. In contrast, structures of PheH lacking the regulatory domain appear to be tetramers. As shown in Figure 1.5, the structure of the "intact" PheH can be re-constructed from these structures, by aligning the catalytic domains. Residues 20-30 form a flexible loop extending over the top of the active site, while the rest of the regulatory domain forms an ACT domain (*29*) with a typical βαββαβ structure (*28*). When the tetrameric structure of PheH is viewed as two dimers, each ACT domain interacts with both catalytic domains in the dimer. Thus, the ACT domains may play a role in maintaining the quaternary structure of PheH.

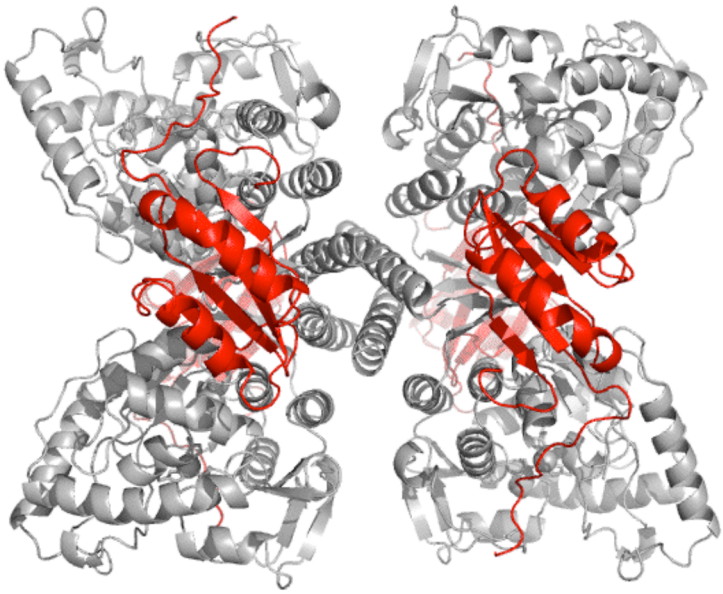

Figure 1.5: The re-constructed structure of PheH. The structure of PheH was built using PDB files 2PAH and 2PHM. The regulatory domain is in red and the rest of the protein in gray.

PheH is the only aromatic amino acid hydroxylase, for which structures with both amino acid and pterin bound are available (*30*). Although not a natural substrate, the amino acid β-thienylalanine has been shown to be able to bind PheH and trigger BH_4 oxidization (*31*). Thus, the structures of PheH with both BH_4 and β-thienylalanine bound can provide significant insight into the substrate binding sites as well as catalysis. As shown in Figure 1.6, BH_4 and β-thienylalanine are separated from each other in the tertiary structure in two different binding pockets. This suggests that there is not a direct chemistry between the two substrates during catalysis, ruling out the hydroxylating intermediate being a pterin derivative. The N(3)-N(5) side of BH_4 faces the iron, and Glu286 is the only amino acid to interact with BH_4 on this side. The importance of Glu286 for BH_4 binding has been demonstrated by mutagenesis. Mutating Glu286 of PheH to alanine increases the K_m value of the pterin by 70-fold (*32*); mutating the corresponding residue in TyrH, Glu332, to alanine increases the K_m value by 10 fold (*33*). BH_4 also interacts with Phe254 by π stacking; mutating the corresponding residue Phe300 to alanine in TyrH decreases the rate constant for pterin oxidization by 5 fold (*34*). The N(1)-N(8) side of BH_4 is hydrogen-bonded with residues Gly247 to Ser251 of a loop. N(8) and the amino group at C(2) of BH_4 are hydrogen-bonded to the backbone carbonyl groups of Leu249 and Gly247, while the side chain at C(6) of BH_4 interacts with the hydroxyl side chain of Ser251. Many 6-substibuted tetrahydropterins can serve as substrates (*5*) of the aromatic amino acid hydroxylases and Ser251 is not a conserved residue in the family, suggesting the interaction with Ser251 is not critical for BH_4 binding.

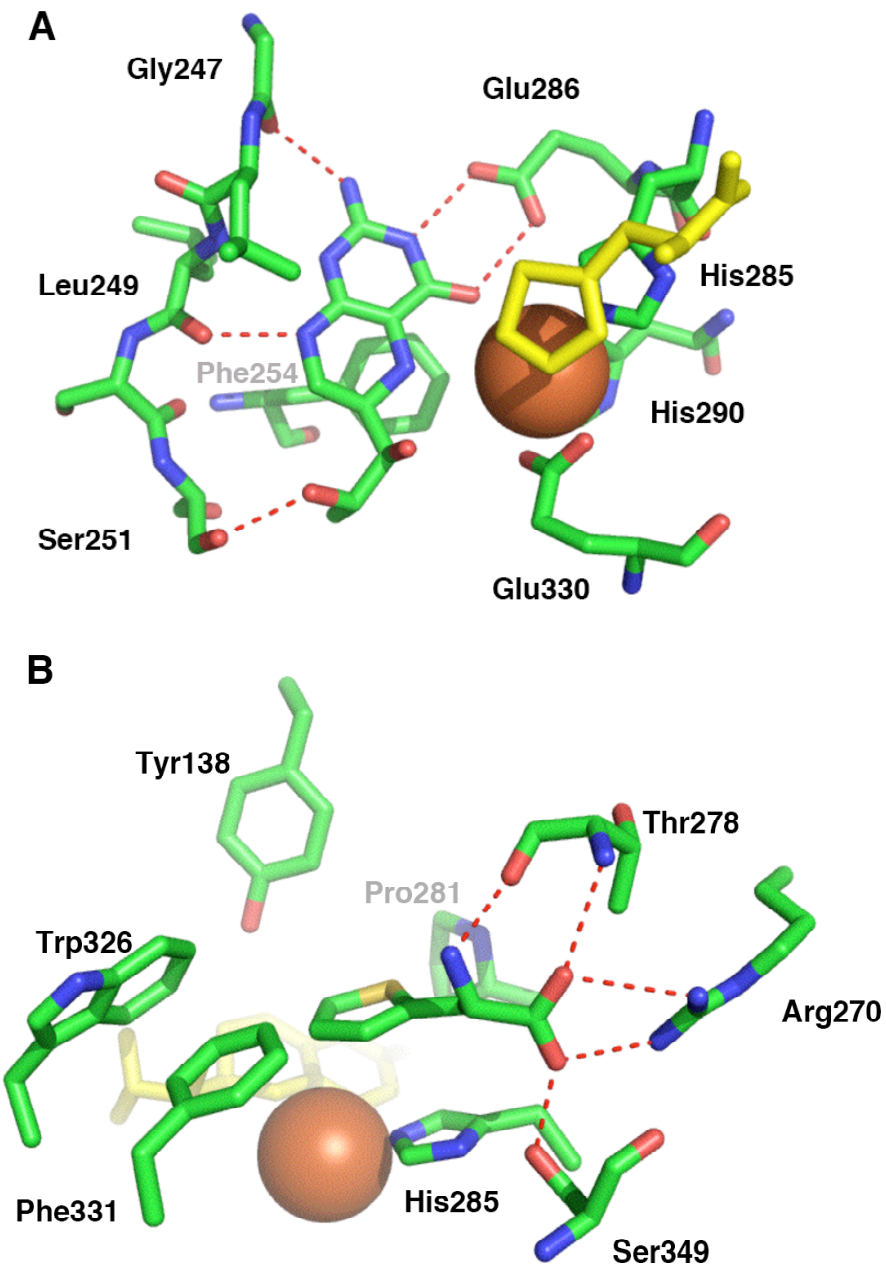

Figure 1.6: BH_4 (A) and amino acid (B) binding sites of PheH (1KW0). A: β-thienylalanine is colored yellow. B: BH_4 is colored yellow.

The amino group of β-thienylalanine interacts with the side chain of Thr278, and the carboxylate group interacts with the amide nitrogen of Thr278, the side chain of Arg270, and the side chain Ser349 (Figure 1.6). The side chain of Arg 270 forms two hydrogen bonds with the carboxylate group of β-thienylalanine; mutating this residue in TyrH to Lys decreases the k_{cat}/K_m value for the amino acid substrate by 4700 fold (*33*). The side chain of the amino acid substrate is held in a hydrophobic pocket consisting of the side chains of Tyr138, Pro281, Trp326 and Phe331.

Deletion of the regulatory domains of the aromatic amino acid hydroxylases yield proteins with the same substrate preferences as the intact proteins (*17, 35, 36*), indicating that all the residues determining the substrate specificity are in the catalytic domains. In light of the high sequence identity, similar structures of the catalytic domains and the similar chemical reactions, the substrate specificities of the aromatic amino acid hydroxylases are likely to be due to small differences in the hydrophobic pocket of the amino acid binding site. Trp326 of PheH is also a tryptophan residue in TyrH, but it is a phenylalanine residue in TrpH; the other three residues of the hydrophobic pocket are more conserved. The bulky side chain of Trp326 of PheH (or TyrH) is a candidate for discriminating phenylalanine (or tyrosine) from tryptophan as a substrate. Mutating the tryptophan to a phenylalanine in PheH yields a protein preferring tryptophan as a substrate to phenylalanine by 30-fold (*37*). However, mutating the corresponding phenylalanine to tryptophan in TrpH yields an enzyme with a similar preference for phenylalanine or tryptophan (*37*), and the same mutation in TyrH does not cause a change of substrate preference (*38*), indicating that the discrimination for

tryptophan as a substrate is not totally dependent on whether phenylalanine or tryptophan is at this position. This also suggests that residues outside of the hydrophobic pocket are also involved in substrate specificity in TyrH. Most of the non-conserved residues in the second sphere of the active site are in loops. There are four loops at the entrance of the active site in PheH (also in TyrH and TrpH), 131-147, 244-251, 270-282 and 375-343. Loop 244-251 packs against the pterin far away from the amino acid binding site and this loop is well conserved (except residue 251 at the very end). Thus, it is unlikely to be related to amino acid specificity. The residues of the other three loops (especially the center residues) are not conserved across the aromatic amino acid hydroxylase family, but are well conserved for each aromatic amino acid hydroxylase. Loop 131-147 undergoes a dramatic conformational change when both pterin and amino acid are bound to PheH; the center residue of the loop, Tyr138, moves more than 10 Å from the surface of the protein into the active site. The corresponding loop in TyrH, 177-193, is also critical for catalysis (*39*). Mutations switching the center residues of this loop in TyrH and PheH did not alter the substrate specificity (*39*). Swapping of the center residue of loop 270-282 or/and 375-343 of PheH with the corresponding residue in TyrH causes dramatic effects on substrate preference. H264Q/V379D PheH has a decrease in preference for phenylalanine versus tyrosine as a substrate by 3000-fold (*40*), although phenylalanine is still preferred over tyrosine. In contrast, D425V TyrH (corresponding to V379D PheH) and Q310H TyrH (corresponds to H264Q PheH) have a preference of tyrosine to phenylalanine as a substrate (*40*), with the former having a 8000-fold preference of phenylalanine to tyrosine and the latter having 35-fold. These

results indicate that the packing of second sphere residues shapes the substrate-binding pocket and contributes to the substrate specificity.

MECHANISM

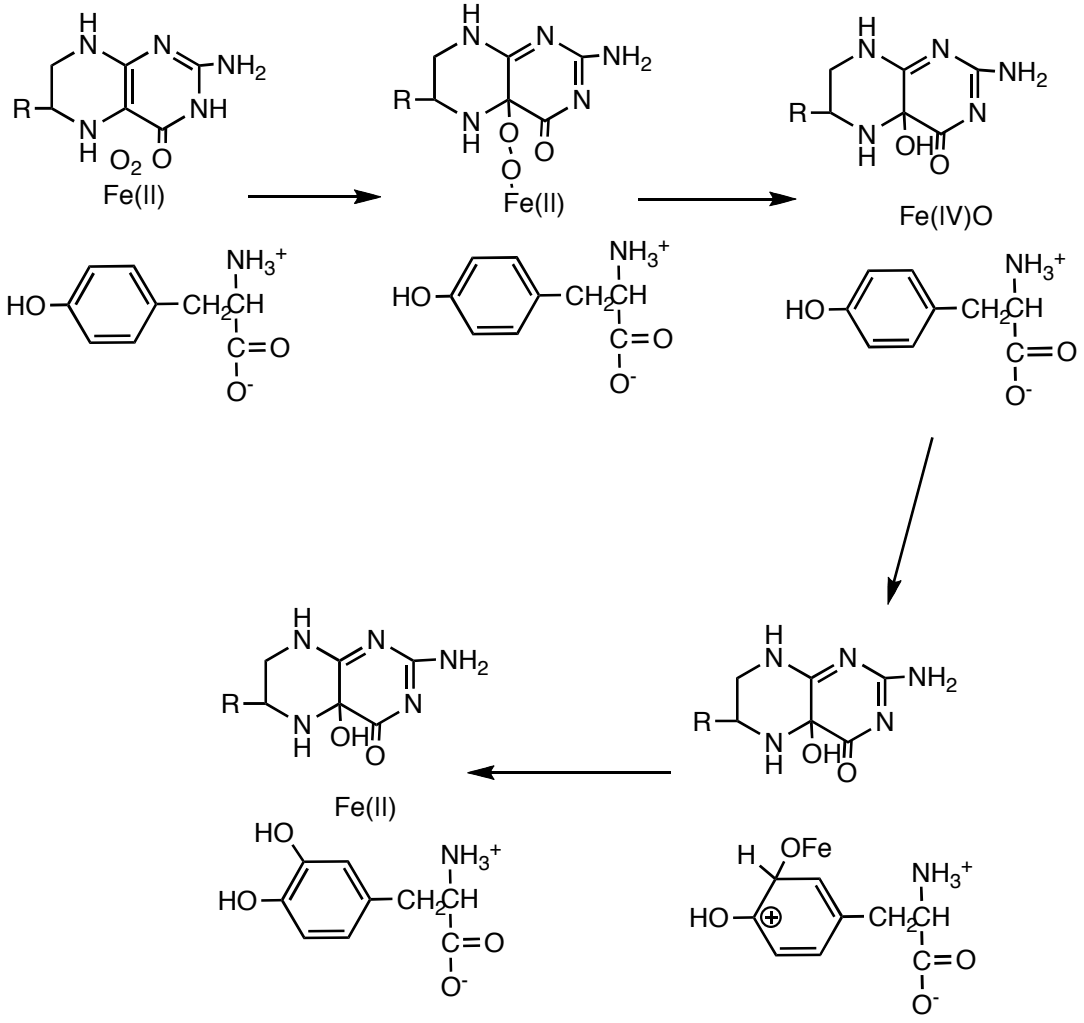

Figure 1.7: Proposed chemical mechanism of TyrH (*21*).

Tyrosine hydroxylase is the best mechanistically characterized enzyme in the aromatic amino acid hydroxylase family (*21, 41*), and the proposed mechanism is shown in Figure 1.7. Catalysis only occurs after all the substrates are bound. The binding of substrates is ordered. Pterin binds first, followed by molecular oxygen and then tyrosine (*41*).

The oxygen atom of the 4a-hydroxy pterin product comes from molecular oxygen (*42*), suggesting there is a direct reaction between molecular oxygen and BH_4. The presence of a peroxy-pterin intermediate has been proposed based on the results of tetrahydropterin autoxidation, in which quinonoid dihydropterin and H_2O_2 are formed as products. The formation of a peroxypterin intermediate is also suggested in the enzyme-catalyzed reaction, in that when tyrosine is used as a substrate for PheH, the hydroxylation of tyrosine is slow while the consumption of tetrahydropterin is much faster and yields H_2O_2 (43). The formation of the hydroxylating intermediate has been suggested to be the first irreversible step based on an ^{18}O kinetic isotope effect of 1.0175 on k_{cat}/K_{O2} (*44*). The peroxypterin cannot serve as the direct hydroxylating intermediate, because this would require breakage of the peroxy O-O bond and hydroxylation of the amino acid in a concerted step. As a result, the amount of pterin oxidized would always equal the amount of amino acid hydroxylated. S395A TyrH has ~1% wild-type activity in terms of formation of DOPA, but this mutant retains the wild-type enzyme activity in terms of formation of the hydroxypterin (*45*). Similar to this, using phenylalanine as a substrate, TyrH consumes pterin faster than tyrosine. These results suggest that the hydroxylating intermediate is formed after the formation of peroxypterin.

Compared with autoxidation of pterin, the enzyme-catalyzed oxidization of pterin is much faster, suggesting that iron of the active site is facilitating the reaction between molecular oxygen and pterin. The geometry and electronic structure of the active site iron have been studied using X-ray absorption spectroscopy (XAS) and magnetic circular dichroism (MCD). The iron of resting PAH (ferrous enzyme with no ligand) is six coordinate (6C), while it becomes five coordinate (5C) after phenylalanine and pterin binding (*46*). Thus, the opening of the coordination position is likely to make room for the reaction with molecular oxygen. The coordination states of the active site iron of PheH were later supported by the X-ray structure, in which the resting PheH is coordinated by three water molecules, two histidines and one glutamate; amino acid and pterin bound PheH is five coordinate due to the lost of two water molecules and the glutamate switching to bidentate coordination (*30, 47*). Similar studies have been performed on TyrH, although a structure of ferrous TyrH is not available. The structure of ferric TyrH with or without a dihydrobiopterin bound shows a five coordinate iron, with two water molecules, two histidines and one glutamate (*14*), but studies using XAS show that the ferrous TyrH with or without a BH_4 bound is six coordinate (*48*). MCD and XAS also show that the iron of the resting TyrH is six coordinate and either tyrosine binding or pterin binding does not alter the coordination state (*49*). However, when both tyrosine and pterin are bound to TyrH, the iron is five coordinate (*49*). Extended X-ray absorption fine structure spectroscopy (EXAFS) further confirms that TyrH with both tyrosine and pterin bound is coordinated by one water molecule, two histidines and one bidentate glutamate (*49*), consistent with the crystal structure of PheH (*30*). The

coordination change of the active site iron is similar to other non-heme iron oxygenases and it facilitates the activation of molecular oxygen (*50-52*).

The coordination of molecular oxygen to the iron and the formation of a peroxypterin intermediate led to the proposal of a Fe(II)-peroxypterin species as an intermediate (Figure 1.7); this subsequently forms a Fe(IV)O hydroxylating intermediate after O-O bond cleavage (*42*) (Figure 1.7). When H_2O_2 is used in place of pterin and oxygen, all three enzymes can hydroxylate phenylalanine into tyrosine (*53*), further supporting that the hydroxylating intermediate is only formed after the cleavage of O-O bond of peroxy-peterin. The hydroxylation of phenylalanine does not occur in the apo-enzymes, establishing a requirement for iron to form the hydroxylating intermediate (*53*). Recently, the presence of a Fe(IV)O intermediate during catalysis of TyrH was directly detected by rapid freeze-quench Mössbauer spectroscopy, with the spectrum resembling Fe(IV)O intermediates in other iron-containing non-heme dependent enzymes (*54*).

The presence of a high valent Fe(IV)O intermediate suggests electrophilic hydroxylation of the amino acid. The deuterium kinetic isotope effect on k_{cat} is unity for TyrH and PheH (*55*), indicating that this chemical step is not rate-limiting (*55*). However, an inverse kinetic isotope effect of k_{cat} (0.93) was observed when 5-^{2}H-tryptophan was used as a substrate for TrpH. Similarly, mutants of TyrH (H336E TyrH) and PheH (V379D PheH and I234D CvPheH) show an inverse deuterium kinetic isotope effect on k_{cat} (*56, 57*). The inverse kinetic isotope effect suggests that the hybridization state of the carbon undergoes an sp^2 to sp^3 transition upon the addition of oxygen.

Further support for an electrophilic mechanism came from the partitioning of 4-substitued phenylalanines as substrates for TyrH (*58*). The ρ values of tetrahydrobiopterin and 6-methyltetrahydroptein were around -5 (*58*), indicating the formation of a very electron poor intermediate after the reaction with the Fe(IV)O intermediate. The most consistent explanation for all these results is the formation of a carbocation upon the reaction of the Fe(IV)O intermediate with the amino acid. This is followed by a 1,2-hydrogen shift at the site of hydroxylation. This shift had been observed decades ago using isotopically labeled substrates (*59*).

The formation and decay rate constants of the Fe(IV)O intermediate are 24 s^{-1} and 35 s^{-1} respectively at 5 ^{o}C determined by rapid freeze-quench Mössbauer spectroscopy during the first turnover (*54*), much faster than k_{cat} (~ 0.9 s^{-1}) during state-state catalysis (*54*). This indicates that chemistry is not the rate-determining step of the reaction. The viscosity effect on k_{cat} is near unity during steady-state analysis (*60*), suggesting the reaction is diffusion-limited. The rapid chemical-quench experiment on TyrH reveals an initial burst during the first few turnovers, suggesting the rate-limiting event is after chemistry (*60*). Thus, the rate-limit step during catalysis of TyrH is product release.

REGULATION

TyrH is regulated long-term at the gene-expression level and short-term at the level of enzyme activity (*4, 61*). The latter includes feedback inhibition by catecholamines and activation by phosphorylation or binding with other proteins (*5, 61*).

There are four phosphorylation sites on the N-terminal regulatory domain of rat TyrH, Ser8, Ser19, Ser31 and Ser40 (*62, 63*). Position 8 is a threonine residue in human TyrH, and the importance of phosphorylation at this position is still not clear. To date, all mammalian TyrH from different species contain those four sites, suggesting all four phosphorylation sites have regulatory importance. PKA phosphorylates Ser40 specifically in vitro (*62, 63*); in vivo, an increase in the concentration of cAMP leads to increased phosphorylation at Ser40 (*62, 63*). Calcium and calmodulin dependent protein kinase II (CaMKII) phosphorylates Ser19 of TyrH in vitro (*64*); in vivo, an increase in the calcium concentration increases the level of Ser19 phosphorylation (*65, 66*). CaMKII is not specific to Ser19; it also phosphorylates Ser40 both in purified TyrH (*64*) and in vivo (*65*). The MAP-activated protein kinases ERK 1 and 2 phosphorylate Ser31 of purified TyrH (*63, 66*); in vivo, the ERK1/2 activators phorbol esters and nerve growth factor increase the level of Ser31 phosphorylation. ERK2 can also phosphorylate Ser8, but much slower than Ser31 (*67*). Protein phosphatase 2A (PP2A) can dephosphorylate Ser19, Ser31 and Ser40 (*61*), while protein phosphatase 2C (PP2C) can dephosphorylate Ser19 and Ser40 (*61*).

Phosphorylation does not have direct effects on the catalytic activity in the absence of other ligands (*61, 64, 68-70*). Consistent with this, deleting the N-terminal

regulatory domain of TyrH yields a fully active protein (*35*), suggesting that phosphorylation does not directly activate TyrH. Instead, phosphorylation regulates the enzyme activity by modulating the interaction of TyrH with other ligands. Phosphorylation of Ser19 or Ser31 has been reported to increase the rate constant for Ser40 phosphorylation (*71-73*) and to increase the stability of TyrH (*71, 72, 74*). In addition, phosphorylation of Ser19 of TyrH is required for 14-3-3 protein binding (*75*). The binding of 14-3-3 proteins decreases the solvent accessibility of Ser19 and Ser40 of TyrH, decreasing the rate of dephosphorylation at those positions by phosphatases (*72, 76*). The function of Ser40 phosphorylation is better understood; it activates TyrH by decreasing the binding affinity of catecholamines by several hundred-fold (*77-79*).

The regulation of TyrH by catecholamine binding and Ser40 phosphorylation is shown in Figure 1.8; the active enzyme, which contains a ferrous iron, catalyzes the hydroxylation of tyrosine into DOPA. The ferrous enzyme can be oxidized to the ferric enzyme (*80*), which is either reduced back to the ferrous form by the substrate BH_4 or bound tightly with a catecholamine. Catecholamines bind to ferric TyrH with affinities of ~ 1 nM (*78*), and this tight binding prevents the reduction of TyrH to the ferrous form, keeping the enzyme in an inactive form. Ser40 phosphorylation increases the dissociation rate constant for a catecholamine by nearly three orders of magnitude (*78, 79*), so that the catecholamine can dissociate from the active site, followed by the rapid reduction to the ferrous form (*80, 81*).

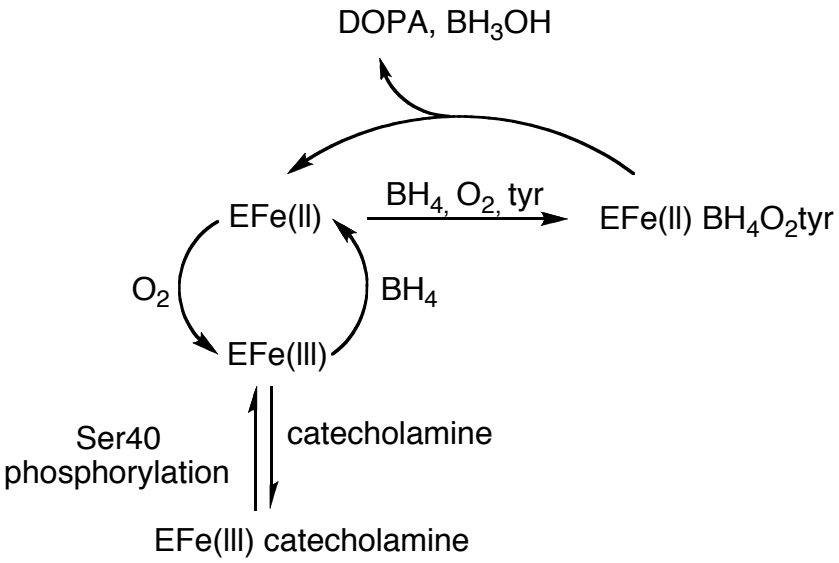

Figure 1.8: Regulatory mechanism of TyrH (*78*).

Structural changes that accompany regulation of TyrH have been suggested by the fact that catecholamine-bound TyrH is more stable than the resting TyrH (*82*), while Ser40-phosphorylated TyrH has decreased stability (*83-85*). Studies using limited-proteolysis showed that dopamine binding causes residues 33-50 to be less susceptible to trypsin digestion, while Ser40 phosphorylation makes the same region more susceptible to digestion (*86*). Consistent with this, binding of dopamine decreases the rate constant for Ser40 phosphorylation (*77*). Gel-filtration chromatography showed that dopamine-bound TyrH has a longer retention time than that of TyrH alone, while Ser40-phosphorylated TyrH has a slightly shorter retention time (*71*). These results not only confirm that the conformational changes occur upon regulation, but also suggest that opposite conformational changes occur upon dopamine binding and Ser40 phosphorylation. To date, a crystal structure is not available for the regulatory domain of

TyrH. There are structures available of the catalytic domain of PheH with a catecholamine bound. This can be used to envision the binding of catecholamines to the catalytic domain of TyrH. The main interaction between the catalytic domain of PheH and catecholamines is between the two hydroxyl groups of the catechol and the active site ferric iron. The amine group protrudes out of the active site without any interaction with the catalytic domain. This suggests that there are interactions between the amino group and the regulatory domain of TyrH, and catecholamine binding or Ser40 phosphorylation of TyrH is likely to modulate this interaction to regulate the affinity of catecholamines.

In contrast to TyrH, the activity of PheH can be modulated by its substrates; the enzyme is inhibited by pterin and activated by phenylalanine. When an assay of purified PheH is initiated by adding enzyme, the rate of tyrosine formation is much slower for the first few minutes (*87*). Pre-incubating PheH with phenylalanine can eliminate this slow phase (*87*), while pre-incubation with BH_4 will prolong this phase (*87*). Thus, BH_4 and phenylalanine shift PheH between an active form and an inactive form. The proposed regulation of PheH by BH_4 and phenylalanine (*87*) is summarized in Figure 1.9: the resting enzyme is in an inactive form; the binding of phenylalanine shifts it to an active form, while BH_4 binding prevents PheH from activation.

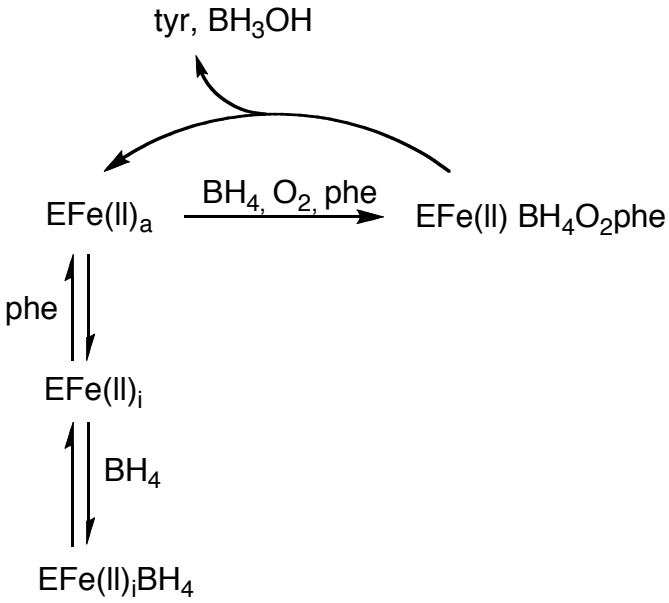

Figure 1.9: Regulatory mechanism of PheH (*87*).

The activity of PheH can also be increased by phosphorylation of the N-terminal regulatory domain at Ser16. Ser16 of PheH can be phosphorylated either by PKA (*88*) or CaMPK (*89*). The enzyme activity is increased less than three-fold after phosphorylation (*90*). More importantly, upon Ser16 phosphorylation, PheH is activated more rapidly upon phenylalanine binding and requires a lower concentration of phenylalanine for activation (*91, 92*), suggesting that Ser16 phosphorylation and phenylalanine binding activate PheH synergistically. Structures of PheH both before and after phosphorylation are available and the two structures are identical, with the first eighteen residues missing in both. This suggests that Ser16 phosphorylation induces only small structural changes before residue 19 or that proteolysis removed these residues before PheH being crystallized. Mutating Ser16 to aspartate or glutamate has same effects on PheH as phosphorylation (*90*), indicating that the charge is responsible for the effect of phosphorylation.

The truncation of the N-terminal regulatory domain can also eliminate the slow phase of tyrosine formation (*17, 93*), suggesting that the regulatory domain is behaving as an inhibitory fragment. The crystal structure of PheH with both the regulatory domain and the catalytic domain should represent the inactive PheH; while the crystal structure of the PheH without the regulatory domain should represent the active PheH. The structures of the catalytic domains in the two cases are overlapping, suggesting the movement of the regulatory domain is responsible for activation by phenylalanine. In the crystal structure of PheH, part of the N-terminal regulatory domain covers the active site

cleft, suggesting that the regulation of PheH activity modulates substrate entry to the active site.

HDMS experiments on PheH in the presence or absence of 5 mM phenylalanine show that several peptides both in the regulatory domain and the catalytic domain have increased deuterium incorporation upon phenylalanine binding (*94*). Most of those peptides are at the interface of the two domains and the active site entrance; however, the residues of the regulatory domain covering the active site do not show a change in deuterium incorporation. The results suggest that a global conformational change of PheH has occurred upon phenylalanine binding. The parallel experiment using the catalytic domain of PheH (truncating the first 117 residues) only shows changes in the peptides in the amino acid binding site. The results do not indicate where the phenylalanine binds to trigger the conformational changes, but a second binding site for phenylalanine other than the active site is likely.

CHAPTER II

IDENTIFICATION OF STRUCTURAL CHANGES ASSOCIATED WITH REGULATION OF TYROSINE HYDROXYLASE BY HYDROGEN/DEUTERIUM EXCHANGE MASS SPECTROMETRY*

Tyrosine hydroxylase (TyrH[1], E.C. 1.14.16.2) catalyzes the conversion of tyrosine into dihydroxyphenylalanine (DOPA), the first and rate-limiting step of catecholamine biosynthesis. TyrH belongs to the small family of aromatic amino acid hydroxylases, which also includes phenylalanine hydroxylase (PheH) and tryptophan hydroxylase (TrpH) (*5*). All three enzymes hydroxylate their respective substrate using tetrahydrobiopterin and molecular oxygen. Phenylalanine hydroxylase is the first and rate-limiting enzyme for phenylalanine catabolism, and tryptophan hydroxylase is the first and rate-limiting enzyme of serotonin biosynthesis. As a result, all three hydroxylases are subject to regulation. In light of the similar reactions they catalyze and their high structural similarity (*13, 14, 22*), they are believed to have the same enzymatic mechanism (*21*). The mammalian forms of these hydroxylases are tetramers (*18, 95, 96*) containing a regulatory domain (100-150 amino acids) at the N-terminus and a larger catalytic domain (around 350 amino acids) at the C-terminus (*15, 17, 19, 35, 36*). The catalytic domains are homologous (*15*), while the regulatory domains are distinct (*15, 16*), probably due to the different regulatory mechanisms.

---

*Reproduced with permission from Wang, S., Sura, G. R., Dangott, L. J., and Fitzpatrick, P. F. (2009) Identification by hydrogen/deuterium exchange of structural changes in tyrosine hydroxylase associated with regulation, *Biochemistry 48*, 4972-4979.

TyrH is regulated by feedback inhibition by catecholamines and phosphorylation of serine residues in the regulatory domain (*77, 97*). TyrH contains a non-heme iron atom in the active site cleft that must be in the ferrous form for activity (*12*). The ferrous enzyme is readily oxidized to the ferric form (*80, 81*), and dopamine binds to the ferric enzyme with a dissociation constant of ~ 1 nM (*78, 79*). Phosphorylation of Ser40 activates TyrH by increasing the dissociation constant for dopamine ~ 500 fold (*78*). Although the structural basis for the regulatory effect is not known, conformational changes upon dopamine binding and phosphorylation of TyrH have been suggested. Limited proteolysis with trypsin showed that dopamine binding protects a region on the regulatory domain of TyrH, and Ser40 phosphorylation makes this region more susceptible to trypsin degradation (*86*). TyrH phosphorylated at Ser40 has a shorter retention time on gel filtration chromatography compared to TyrH alone, and dopamine-bound TyrH has a slightly longer retention time (*71*). Until now the only structures available for TyrH are the catalytic domain with and without 7, 8-dihydrobiopterin bound (*14, 98*). To probe the effects of dopamine binding and phosphorylation on the structure of TyrH, hydrogen deuterium exchange mass spectrometry was used. The results are described here.

EXPERIMENTAL PROCEDURES

Materials. Dopamine and ATP were from Sigma-Aldrich Chemical Co. (Milwaukee, WI). Porcine stomach pepsin A was from Worthington Biochemical Co. (Lakewood, NJ). Deuterium oxide (D_2O, 99% D) was from Cambridge Isotope Laboratories (Andover, MA). HPLC grade water was from Mallinckrodt Chemical Inc. (St, Louis, MO), and HPLC grade acetonitrile was from VWR-International (Darmstadt, Germany). Formic acid was from Michrom Bioresources Inc. (Auburn, CA). All other chemicals were of the highest purity commercially available.

Protein purification. The catalytic domain of cAMP dependent protein kinase (PKA) from beef heart was purified according to Flockhart et al (*99*). Rat tyrosine hydroxylase was purified as previously described (*33*). Phosphorylation of TyrH was performed as previously described (*78*) with minor modifications. Approximately 10 ml of TyrH (20 μM) in 50 mM Hepes, 200 mM KCl, and 10% glycerol, pH 7.3, was incubated with 50 μM ATP, 6 mM $MgSO_4$, 2 μg/ml PKA at 4 ^oC for 1 h. An additional aliquot of ATP was added to give a concentration of 100 μM, followed by another 1 h incubation. The degree of phosphorylation was monitored using a MonoQ column as previously described (*78*). The phosphorylated TyrH was purified using a Q-Sepharose column. To ensure that the enzyme contained a stoichiometric amount of ferric ion, an equimolar amount of Fe $(NH_4)_2$ $(SO_4)_2$ was added to purified TyrH or phosphorylated TyrH, followed by Q-Sepharose chromatography. The purified protein was stored in 10% glycerol, 200 mM KCl and 200 mM Hepes (pH 7.3) at a concentration of ~ 0.3 mM at -80 ^oC.

To obtain the TyrH-dopamine complex, dopamine was added to 0.3 mM TyrH in 10% glycerol, 200 mM KCl and 200 mM Hepes (pH 7.3) to a final concentration of 0.5 mM. The binding of dopamine to TyrH was monitored by following the absorbance increase at 690 nm; the binding reaction was complete after 30 minutes at 4 ^{o}C.

Hydrogen/deuterium exchange and mass spectrometry. The exchange reaction was initiated by diluting 25 µl of 0.3 mM enzyme with 500 µl of D_2O buffer (200 mM Hepes, pD 7.7) at 25 ^{o}C. Over the time course of the experiment, 20 µl aliquots were taken and quenched with 20 µl of 300 mM H_3PO_4 in H_2O at 4 ^{o}C to lower the pH to 2.4. The quenched sample was immediately frozen with liquid nitrogen and stored at -80 ^{o}C for less than 24 h. Samples were thawed quickly and pepsin (15 mg/ml) was added to yield ratios of pepsin to TyrH (w/w) of 0.5, 1 or 2. The first 3 min of the pepsin digestion was performed on ice and the last 2 min of digestion was performed in the 20 µL HPLC injection loop, which was submerged in ice. The resulting peptides were then injected onto a Vydac C_{18} column (2.1 mm × 150 mm) connected to a Thermo Finnigan HPLC system. Most of the HPLC system was kept at 4 ^{o}C, including the injection loop, the tubing, the C_{18} column and the solvents. After a 3 min desalting with 98% solvent A (0.3% formic acid in H_2O, pH 2.4) and 2% solvent B (0.3% formic acid in acetonitrile, pH* 2.4) at a flow rate of 300 µl/min, a gradient of 10 – 60 % solvent B over 9 min was applied at a flow rate of 200 µl/min. Most of the peptides were eluted at 15% to 50% acetonitrile within 6 min. The outflow from the HPLC column was injected directly into a Thermo Finnigan LCQ DECA XP ion-trap mass spectrometer. Singly, doubly and triply charged peptides, with m/z values of 400 to 2000, were analyzed.

To identify peptides, an independent tandem mass spectrometry (MS/MS) experiment was performed using the same digestion and elution conditions, except that H_2O instead of D_2O was used in the dilution step. Peptide assignment was performed using the program TurboSEQUEST (Thermo Finnigan, version 3.1).

To obtain fully-deuterated peptides, 10 µl of 0.3 mM TyrH was diluted with 200 µl of 200 mM Hepes buffer (pH 7.3) in H_2O and 210 µl of 300 mM H_3PO_4 in H_2O at 4 ^oC. Pepsin was added to give pepsin to protein ratios (w/w) of 1 or 2. After 5 min on ice, three 50 µl aliquots were taken out and loaded onto three 500 µl Bio-Spin 6 columns to isolate the peptic peptides. To remove the pepsin, the columns were centrifuged at 1,000 g for 30 s; the flow through was discarded. To collect the peptides, each column was washed with 300 µl D_2O and centrifuged at 1,000 g for 60 s. The washing was repeated twice, and all the flow through was combined. The pooled samples were lyophilized. The resulting peptides were resuspended in 20 µl D_2O and heated to 90 ^oC for 90 min. After cooling, 5 µl of 500 mM phosphate buffer in D_2O (pD 2.8) was added. Twenty µl of the peptides was loaded onto the HPLC, and peptide separation and analysis were performed as described above. Only 21 peptides were found with good spectra, suggesting that there was peptide loss due to the extra steps to obtain fully deuterated peptides. Under the experimental conditions, the back-exchange level of the 21 well-resolved peptides was ~ 35%. As a result, a value of 35% back exchange was used for the rest of the peptides.

Data analysis. The .raw MS files were processed using the Thermo Finnigan Xcalibur software. The spectra of individual peptides were transferred to Excel, and

centroid data were identified using the program HX-Express (*100*); the program MagTran (*101*) was also used for the peptides showing altered exchange behaviors and gave the same results as HX-Express. The deuterium content of individual peptides was calculated using Equation 2.1, where M_t is the measured mass of the peptide at time t; M_H is the measured mass of the nondeuterated peptide; M_D is the measured mass of the completely deuterated peptide corrected for back-exchange. The time course for deuterium incorporation of each peptide was fitted to Equation 2.2 or linearly, where N is the number of exchangeable amide hydrogens over the time course of the experiment, and A and B are the numbers of amide hydrogens with exchange rate constants k_1 and k_2, respectively.

$$D\% = (M_t - M_H)/ (M_D - M_H) \times 100\% \quad (2.1)$$

$$Y = N - Ae^{-k_1 t} - Be^{-k_2 t} \quad (2.2)$$

Six independent experiments were performed for each condition. Due to the availability of the peptides in different pepsin to protein ratios (w/w), most peptides could be analyzed for four different experiments; all were analyzed in at least two independent experiments with the same pepsin to protein ratio (w/w). The results were well reproducible in independent experiments. The results, including standard deviations indicated in figures were all calculated from the experiments with the same pepsin to protein ratio (w/w).

RESULTS

Identification of peptides. Electrospray mass spectrometry of peptic peptides was used to analyze the extent of deuterium incorporation from solvent into peptide bonds in TyrH under different conditions. Pepsin was used to generate the peptides because it is active at pH 2-3 where back-exchange from the peptide bond to solvent is minimized. In preliminary experiments, the ratio of pepsin to TyrH was varied from 0.5 to 2 (mass/mass). Some different peptides were generated with the different masses of pepsin. Combining the peptides generated at ratios of pepsin to TyrH of 0.5, 1, and 2 allowed reproducible detection of peptides covering ~70% of the protein (Figure 2.1). Most of the residues which were not found in peptide peptides by mass spectrometry were in three regions of the protein: residues 1-27, 143-174, and 191-209. The remainder of the protein is well-covered.

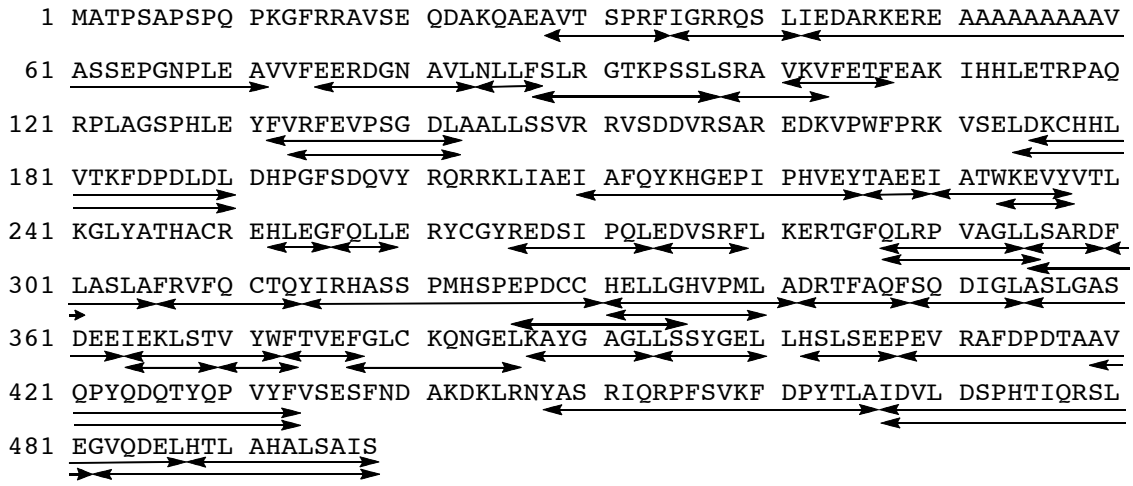

Figure 2.1: Peptic peptides (arrows) of TyrH used in the hydrogen deuterium exchange mass spectrometry experiments.

Amide H/D exchange dynamics of the native enzyme. Figure 2.2 shows the changes in deuterium content of peptides in the catalytic domain at different times of incubation in D_2O; no structure is available for the regulatory domain of TyrH. Figure 2.3 illustrates the three different exchange patterns of peptides. There is a central core around the active site which shows little exchange over the 1 h time course of the experiment: residues 226-259, 300-354, 364-377, and 387-393. The two histidines and one glutamate, which act as iron ligands, are all included in these peptides. Three peptides (28-34, 35-41, 42-71) of the regulatory domain exhibit rapid and complete exchange in less than 10 s, suggesting that this portion of the protein is highly mobile. This region contains two of the phosphorylation sites, Ser 31 and Ser 40. The remainder of the protein shows time-dependent exchange, consistent with EX2 behavior due to transient formation of exchange-competent conformations. Residues in the tetramerization domain, 455-498, show very similar patterns of exchange, suggesting transient dissociation of individual subunits.

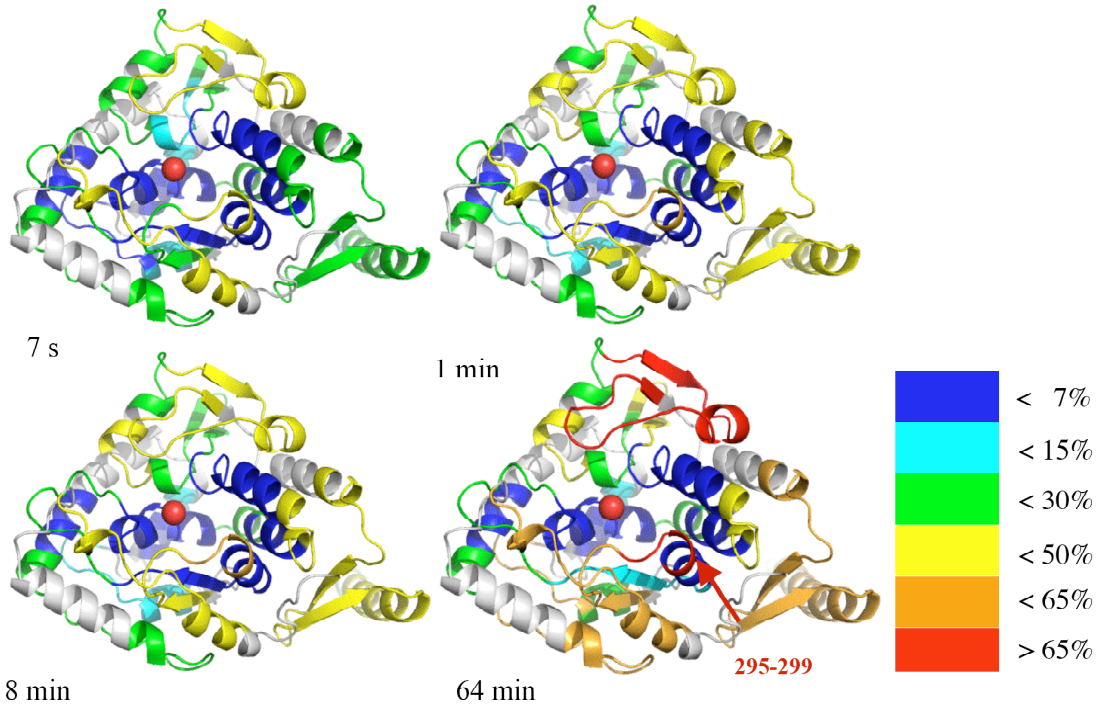

Figure 2.2: The extent of deuterium incorporation into peptides in the catalytic domain of TyrH at various times. Residues are color-labeled according to the deuterium content in the respective peptides. The structure of the backbone of residues 178-199 of TyrH (1TOH) is from the corresponding residues in PheH (3PAH); the iron is shown as a red sphere.

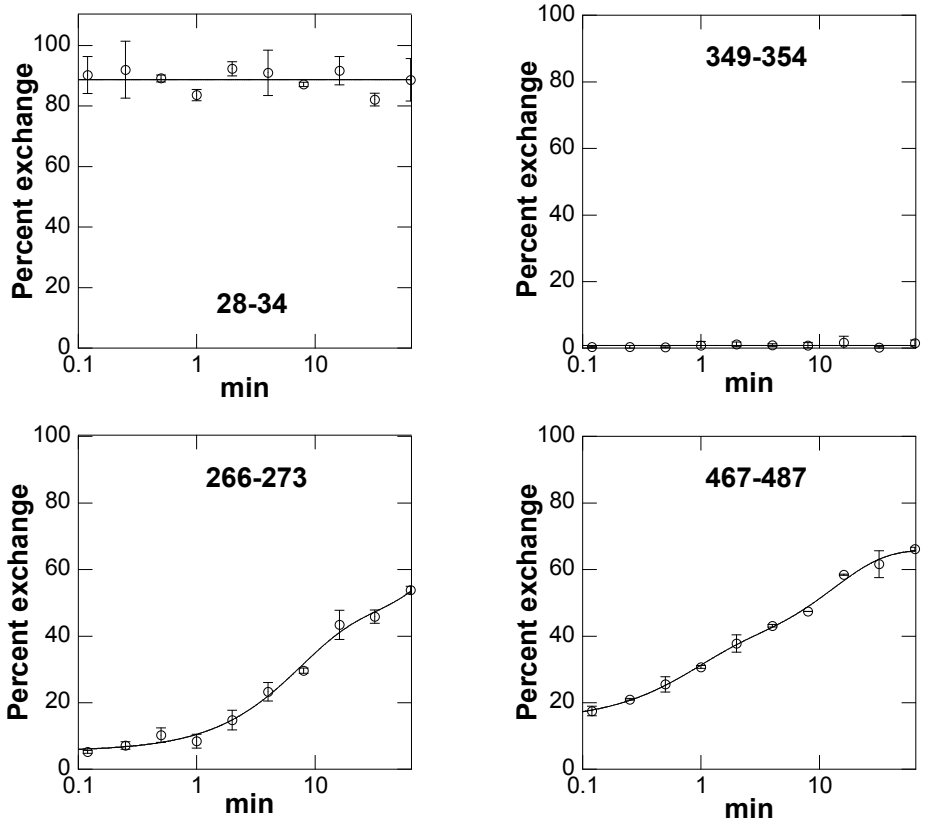

Figure 2.3: Time course of deuterium incorporation into peptides 28-34, 266-273,349-354 and 467-487 for TyrH alone. The lines were obtained by fitting the data to equation 2.2.

A similar analysis was carried with TyrH lacking the regulatory domain, Δ155 TyrH. Almost 80% of this protein could be detected in the mass spectrometer. While there were some differences in the identities of the individual peptides, the overall pattern of exchange was very similar to that seen in the intact protein (results not shown).

Structural changes upon dopamine binding and phosphorylation. The deuterium exchange dynamics of TyrH with dopamine bound or phosphorylated at Ser40 were also examined to gain insight into the structural changes accompanying regulation. The peptides surrounding Ser40, 35-41 and 42-71, were not detected in the phosphorylated protein. The reasons for this were not pursued, but phosphorylated peptides are typically quite difficult to detect by mass spectrometry, and phosphorylation of Ser40 makes this region of the protein more susceptible to proteolysis (*102*). With those exceptions, all of the peptides, which could reproducibly be detected in the native enzyme, could also be detected in the dopamine-bound and phosphorylated forms. Only three peptides show significantly different exchange behavior upon dopamine binding or phosphorylation (Figure 2.4). All three show dramatic decreases in the rates of deuterium incorporation. Two of the fragments (35-41, 42-71) are on the regulatory domain and the other one (295-299) is on the catalytic domain (Figure 2. 2). The altered exchange behavior of peptide 295-299 was confirmed by the overlapping peptide 295-301. The effect of phosphorylation on the exchange kinetics is the opposite, in that peptide 295-299 shows more rapid deuterium incorporation upon Ser40 phosphorylation.

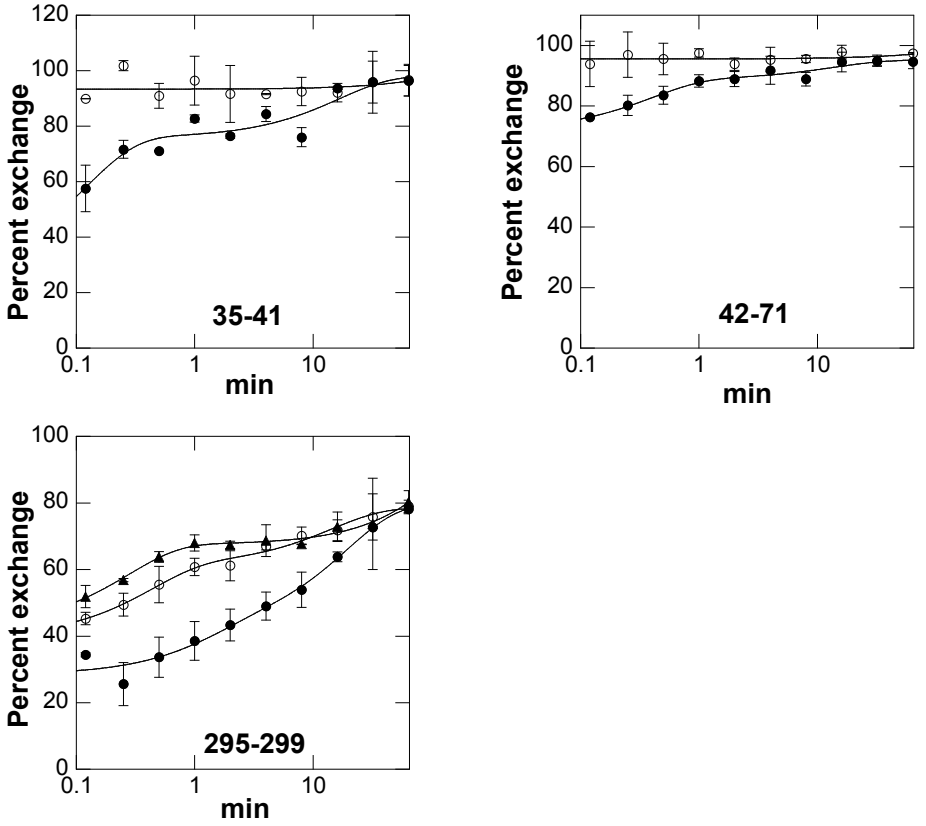

Figure 2.4: Time course of deuterium incorporation into peptides 35-41, 42-72, and 295-299 for TyrH alone (open circles), with bound dopamine (filled circles) or phosphorylated at Ser40 (filled triangles).

DISCUSSION

The present results provide significant insight into the structural changes associated with regulation of TyrH and the conformational flexibility of the enzyme. We found that the conformational changes induced by dopamine binding and Ser40 phosphorylation involve three peptides (35-41, 42-71, 295-299), and dopamine binding and Ser40 phosphorylation have opposite effects on the dynamics of these three peptides.

Phosphorylation-induced local conformational changes near phosphorylation sites have been seen in many regulatory enzymes (*103*), and this has also been suggested to be the case for TyrH (*86*). In our results, residues 35-71 are protected from the solvent upon dopamine binding, agreeing with the limited proteolysis studies that show dopamine binding protects Arg33 and Arg49 (*86*). This result is also consistent with the observation that dopamine binding slows Ser40 phosphorylation (*77*). Although peptides 35-41 and 42-71 were not detected in the phosphorylated protein, Arg33 and Arg49 are more susceptible for proteolysis after phosphorylation at Ser40, in contrast to the effects of dopamine binding (*86*). The isolated catalytic domain of TyrH has a dissociation constant for dopamine similar to that of phosphorylated TyrH (Wang and Fitzpatrick, unpublished observation), suggesting that the regulatory domain is responsible for tight binding of dopamine in the active site. A reasonable explanation for all of the results is that dopamine binding and Ser40 phosphorylation have opposite effects on the structure of the regulatory domain.

The decreased exchange observed upon dopamine binding in respective peptides can be explained by more hydrogen bonding to the amides or/and the amides becoming more buried. Together with the effects on proteolysis and Ser40 phosphorylation rate, a reasonable model to explain the H/D exchange data is that dopamine binding makes the region surrounding Ser40 close down on the catalytic domain so that the amides in this region are more protected from the solvent.

In the catalytic domain, peptide 295-299 was found to have decreased incorporation of deuterium when dopamine is bound to TyrH, and increased deuterium incorporation when TyrH is phosphorylated at Ser40 (Figure 2.4). Peptide 295-299 overlaps with one of the surface loops, 290-296, which is at the entrance of the active (*98*). Of the peptide, four amides in the peptide 295-299, the N-terminal two are in the loop and the other two are at the beginning of a helix. The rest of the helix (300-305) incorporated little or none deuterium under all the three conditions, which indicates that it has little conformational flexibility. Two peptides (287-294, 287-295) on the other end of loop 290-296 were analyzed in this study, but neither shows altered exchange behavior upon dopamine binding or phosphorylation, suggesting that the majority of the loop is not involved in structural changes induced by dopamine binding or phosphorylation. Collectively, the altered exchange behavior of 295-299 is not likely to due to the movement of loop 290-296, since that should change the exchange behavior of peptides 287-294. Rather, the altered exchange pattern of 295-299 can be explained by changed surface exposure due to movement of the regulatory domain. This is

supported by the fact that the maximum exchange content of the peptide during the experimental time-course under the three conditions is the same.

The structures of the regulatory domain and the catalytic domain of PheH are both available, while only the structure of the catalytic domain of TyrH is available. Insight into the structure of the regulatory domain of TyrH can be gained from comparison of the sequences of the two regulatory domains. As shown in Figure 2.5, the sequences of the regulatory domains of PheH and TyrH can be aligned, except that residues 1-28 and residues 49-79 of TyrH do not have corresponding residues on PheH. The phosphorylation sites, Ser40 of TyrH and Ser16 of PheH, are not aligned by the default parameters of Clustal W2. This agrees with the different phosphorylation activation mechanisms, in which Ser40 phosphorylation of TyrH facilitates dopamine dissociation, and Ser16 phosphorylation of PheH reduces the phenylalanine concentration required for substrate activation (*91*). Peptides 35-41 and 42-71 of the regulatory domain of TyrH show altered exchange patterns upon dopamine binding, and residues 35-47 align well with residues 19-31 of PheH. To obtain more structural information about residues 35-71 of TyrH, the structure of PheH containing the regulatory domain and the catalytic domain is used. Figure 2.6 shows that, residues 19-31 of PheH (35-47 in TyrH) lie on top of residues 249-253 (295-299 of TyrH) and partially protects them from the solvent. This explains quite well the H/D exchange patterns of peptides 35-41, 42-71 and 295-299. In the absence of dopamine binding or phosphorylation, residues 35-71 is a labile loop lying on top of 295-299; upon dopamine binding, 35-71 become less labile, restricting the accessibility of solvent both for 295-

299 and for 35-71. Upon Ser40 phosphorylation, 35-71 becomes more flexible, leaving 295-299 more accessible to solvent. The interaction of 35-71 with 295-299 makes TyrH more compact upon dopamine binding, leading to a shorter retention time on gel filtration chromatography and less susceptibility to phosphorylation. In addition, the increased flexibility due to Ser40 phosphorylation makes TyrH more accessible to trypsin for degradation.

```
TyrH     1 MATPSAPSPQ PKGFRRAVSE QDAKQAEAVT SPRFIGRRQS LIEDARKERE 50
PheH     1 ---------- ----MAAVVL ENGVLSRKLS D---FGQETS YIEDNSNQ-- 31

TyrH    51 AAAAAAAAAV ASSEPGNPLE AVVFEERDGN AVLNLLFSLR GTKPSSLSRA 100
PheH    32 ---------- ---------- ---------N GAISLIFSLK -EEVGALAKV 51

TyrH   101 VKVFETFEAK IHHLETRPAQ RPLAGSPHLE YFVRFEVPSG -DLAALLSSV 149
PheH    52 LRLFEENDIN LTHIESRPSR ---LNKDEYE FFTYLDKRSK PVLGSIIKSL 98

TyrH   150 R-----RVSD DVRSAREDKV P 165
PheH    99 RNDIGATVHE LSRDKEKNTV P 119
```

Figure 2.5: Sequence alignment of TyrH and PheH regulatory domains. The default parameters of Clustal W2 (*104*) were used. Identical residues are in bold. The phosphorylation sites, Ser40 of TyrH and Ser16 of PheH, are underlined. Peptides of TyrH which showed altered H/D exchange patterns upon dopamine binding are indicated with arrows.

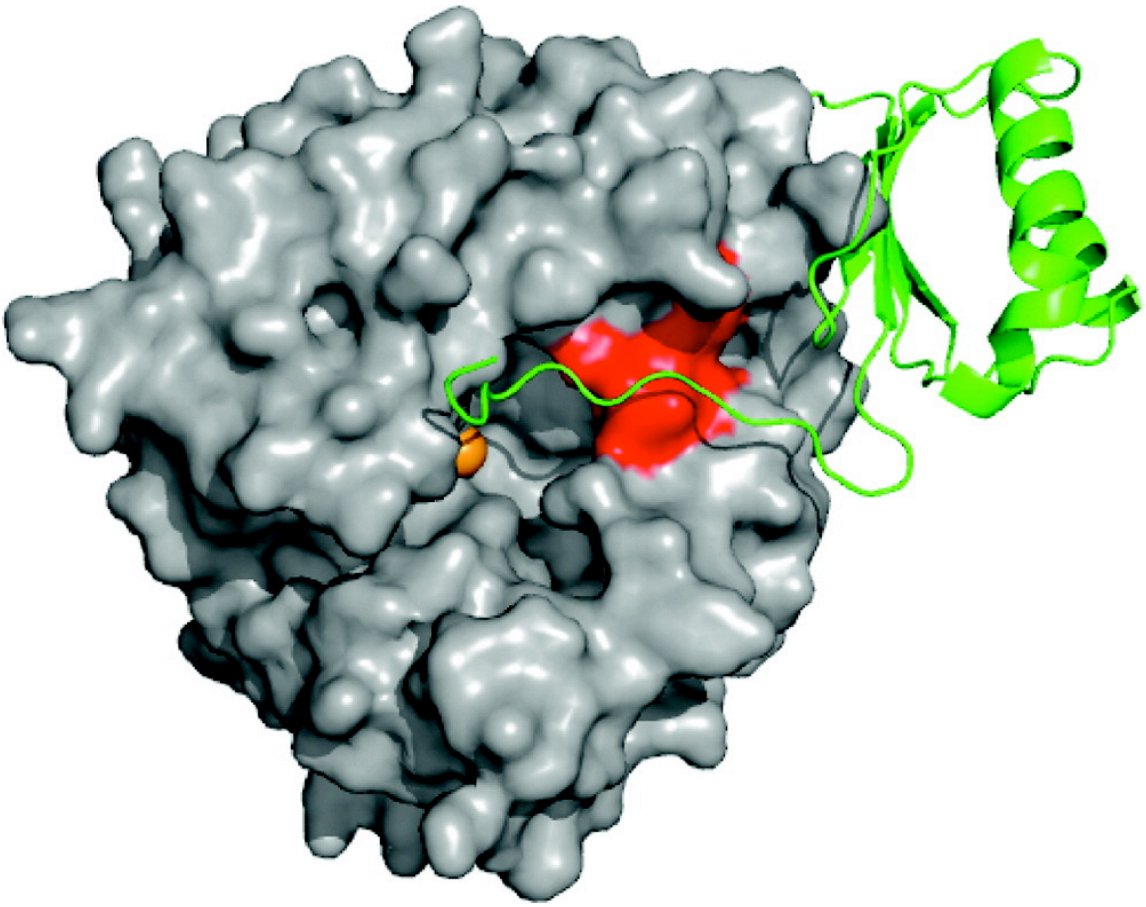

Figure 2.6. Interactions between the regulatory and catalytic domains of PheH. The figure was generated using the PDB file 2PHM. The catalytic domain of PheH is shown as a surface rendering in gray, while the regulatory domain of PheH is shown as a green cartoon. Residues 249-253 are in red. The active site iron is an orange sphere.

The exchange rate of unstructured peptides is ~ 10 s^{-1} (*105*). As a result, the complete exchange of residues 28-71 within 10 s indicates a lack of secondary structure of this region. Peptides after residue 71 in the regulatory domain do not show complete exchange. The isolated TyrH regulatory domain contains a high content of β-sheet structure (*35*), suggesting the β-sheet structure is formed by residues after 71. Residues 80-165 show ~ 25% sequence identity with corresponding residues in the regulatory domain of PheH, which form a two helix and four β-sheet bundle. Residues 80-165 of TyrH may adopt a similar structure to the corresponding residues of PheH.

The majority of the catalytic domain does not show conformational changes upon dopamine binding or Ser40 phosphorylation. There are four loops (177-193, 316-328, 421-429, and 290-296) at the entrance of the active site, and three of them have been shown to be functionally important. Alanine scanning studies showed that loop 178-193 of TyrH is important for catalysis (*39*); fluorescence anisotropy studies showed that this loop becomes more rigid upon pterin binding (*106*). Thus loop 178-193 of TyrH is important for enzyme function. Loops 421-429 and 316-328 are critical for substrate specificity (*40*). When the center residues are mutated to the corresponding residues of PheH, the protein functions more like PheH than TyrH (*40*). There is one more loop (290-296) at the active site entrance. The crystal structure of pterin-bound TyrH shows that this loop may be involved in pterin binding (*98*). In the present study, this loop has been shown to be involved in regulation of TyrH. All four loops show relatively a high percentage of deuterium incorporation, indicating the high dynamics of these loops.

The tetramerization domain is composed of a long helix containing ~ 26 amino acids and a two strand β-sheet. All the peptides in this region have a similar exchange behavior, with time-dependent incorporation of deuterium. The incorporation of deuterium into this region could be due to the transient loosening-up of the helix and the β-sheet. The similar exchange patterns of the helix and the β-sheet indicate that the deuterium incorporation into the helix and the β-sheet is concerted, meaning there is transient dissociation of the tetramer into dimers and monomers.

In conclusion, we have found three peptides in TyrH showing altered exchange patterns upon dopamine binding or phosphorylation. Two are on the regulatory domain surrounding the phosphorylation site Ser40, and the other one is on one of the four loops at the active site entrance. The three peptides show more solvent accessibility upon phosphorylation and less upon dopamine binding.

CHAPTER III

FLUORESCENCE ANISOTROPY REVEALS EFFECTS OF SER40 PHOSPHORYLATION ON THE DYNAMICS OF A REGION IN THE REGULATORY DOMAIN OF TYROSINE HYDROXYLASE

Tyrosine hydroxylase (TyrH) belongs to the non-heme iron-containing aromatic amino acid hydroxylase family (*4, 5*). The enzyme catalyzes the hydroxylation of tyrosine to dihyroxyphenylalanine (DOPA) using molecular oxygen and tetrahydrobiopterin (BH_4). As the first and rate-limiting enzyme in the biosynthesis of catecholamines, regulation of TyrH activity is critical. Feedback inhibition by catecholamines and activation by Ser40 phosphorylation are the best-established regulatory mechanisms (*77, 107*). As shown in Figure 3.1, TyrH converts tyrosine into dihydroxyphenylalanine (DOPA) using a ferrous iron in the active site (*12*). Alternatively, a fraction of the ferrous enzyme can be oxidized to the ferric form (*80, 81*), rendering the enzyme inactive; the ferric enzyme can be reduced by BH_4, making TyrH active again (*81*). The ferric enzyme can also bind catecholamines in the active site, with binding affinities ranging 1-5 nM (*78, 79*). This prevents the reduction by BH_4, trapping the enzyme in an inactive form. This inhibition can be reversed by Ser40 phosphorylation, which increases the catecholamine dissociation rate constant by two to three orders of magnitude (*78, 79*). As a result, catecholamines can dissociate from the active site, allowing TyrH to become active again upon reduction to the ferrous form.

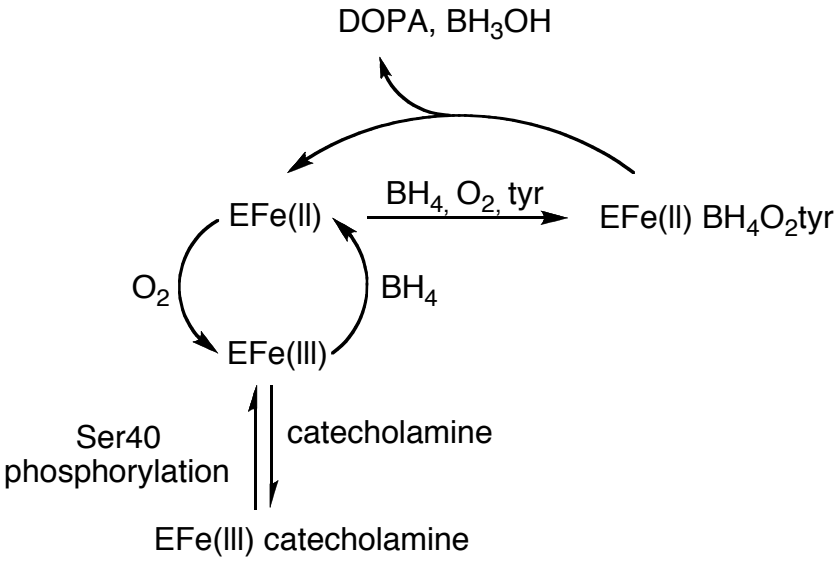

Figure 3.1: Regulation of TyrH.

Previously, hydrogen-deuterium exchange mass spectrometry showed that upon dopamine binding, residues 295-299 at the active site entrance and residues 35-71 in the regulatory domain are protected from exchange (*108*). Phosphorylation of TyrH at Ser40 has the opposite effect on the exchange kinetics of residues 295-299, but residues 35-71 of the phosphorylated enzyme were not detectable by mass spectrometry (*108*). These results led to a model that dopamine binding stabilizes the N-terminus of the regulatory domain of TyrH over the active site entrance, while Ser40 phosphorylation shifts the N-terminus of the regulatory domain away from the active site. The lack of structural information about residues 35-71 in the phosphorylated enzyme makes the understanding of the dynamics of the N-terminus of the regulatory domain incomplete. Thus, a complementary method was required to study the dynamics of this region. Fluorescence anisotropy and quenching are excellent probes of local dynamics in proteins (*109-111*). We have previously shown that mutating all three intrinsic tryptophans in TyrH to phenylalanines has little effect on enzyme activity or substrate binding (*106*). We describe here the use of single tryptophan-containing enzymes to study the effects of phosphorylation on the dynamics of the N-terminus of TyrH.

EXPERIMENTAL PROCEDURES.

Materials. Hepes (4-(2-hydroxyethyl)-1-piperazine ethanesulfonic acid) was obtained from USB Co. (Cleveland, OH). Ultrapure glycerol and N-acetyl-L-tryptophanamide were from Sigma-Aldrich Chemical Co. (St. Louis, MO). All the other chemicals were of the highest purity commercially available.

Protein purification. The plasmid for expression of mutant TyrH with the three intrinsic tryptophans replaced by phenylalanines has been described previously (*106*). The introduction of a single tryptophan at position 14, 34 or 74 was performed by QuikChange site-directed mutagenesis (Stratagene). The purification of the mutant enzymes was modified from that described previously for wild-type TyrH (*93*). After the heparin column, the enzymes were incubated with a 1.2 molar ratio of ferrous iron, followed by further purification with a Q-Sepharose column (10 × 200 mm) (*108*). Phosphorylation and purification of the phosphorylated enzymes were performed as previously described (*78, 108*). The purified protein was dialyzed into 50 mM Hepes, 100 mM KCl and 10% ultrapure glycerol, pH 7.3 for the fluorescence experiments.

Kinetic assays. The enzyme activity was determined using a colorimetric end-point assay at pH 7 and 30 ^{o}C as previously described (*41*). The dopamine dissociation rate constants were determined by monitoring the decrease in absorbance at 550 nm after the enzyme-dopamine complex was mixed with excess dihydroxynaphthalene at pH 7 and 10 ^{o}C as previously described (*78*).

Fluorescence analyses. Steady-state anisotropies and the effects of acrylamide as a quencher were determined on a Koala Spectrophotometer (ISS, Urbana Champaign,

IL) with a 300 W Xenom lamp as the excitation source, using 2-5 μM enzyme in 50 mM Hepes, 10% glycerol and 100mM KCl at 22 ^{o}C. For anisotropy measurements, samples were excited with vertically polarized light at 300 nm with a slit width of 4 nm. The emission intensity of both horizontally (I_H) and vertically (I_V) polarized light were measured, and the anisotropy, *r*, was subsequently calculated using Equation 3.1.For the quenching studies, samples were excited at 300 nm, and the emission intensity, F, was measured with a Schott WG-345 filter at various acrylamide concentrations Q. Subsequently, K_{SV} and k_q were calculated using Equation 3.2 and 3.3, respectively. Here, F_0 is the fluorescent intensity in the absence of acrylamide, K_{SV} is the Stern-Volmer constant, τ is the lifetime of the fluorophore, and k_q is the bimolecular quenching rate constant.

$$r = (I_V - I_H)/(I_V + I_H) \quad (3.1)$$

$$F_0/F = 1 + K_{SV} \times [Q] \quad (3.2)$$

$$K_{SV} = k_q \times \tau \quad (3.3)$$

Lifetime and dynamic anisotropy experiments were performed using a K2 fluorometer with multi-frequency phase and modulation (ISS, Urbana Champaign, IL). The excitation light of 300 nm was generated from a light-emitting diode, and the emission was collected through a Schott WG-345 filter and a polarizer at an angle of 35^{o}. An N-acetyl-L-tryptophanamide (NATA) solution in 5 mM sodium phosphate (pH 7.0) was used as reference with a lifetime of 2.85 ns. Data were collected between 1 and 250 MHz. The calculations of the lifetimes were performed using a continuous Lorentzian distribution model, since it gave the best χ^2 value for all the conditions.

Analyses of the dynamic anisotropy data were performed using the software from Global Unlimited (Urbana Champaign, IL).

RESULTS

Activities of single-tryptophan enzymes. There are three tryptophan residues in TyrH, at positions 166, 233 and 372. Mutation of all three to phenylalanine yields a tryptophan-free enzyme (F_3W TyrH) with wild-type enzyme activity (*106*). Three single tryptophan-containing enzymes were constructed by replacing each of the three aromatic amino acids in the regulatory domain of F_3W TyrH, Phe14, Phe34 and Phe74, with tryptophan, yielding F14W/F_3W TyrH, F34W/F_3W TyrH and F74W/F_3W TyrH. The mutant enzymes have comparable k_{cat} and K_m values to wild-type TyrH (Table 3.1), suggesting that catalysis and substrate binding are not altered by the mutations. The dopamine dissociation rate constants were used as an indicator of the regulatory function of the mutants. Dopamine binds to TyrH to form a greenish complex, with an absorption maximum of 690 nm, whereas dihydroxynaphthalene (DHN) binds to TyrH to form a complex with an absorption maximum of 550 nm. As a result, the increase of absorbance at 550 nm when a large excess of DHN is added to the enzyme-dopamine complex can be used to measure the dopamine dissociation rate constant. Adding DHN to the dopamine complexes of the unphosphorylated mutant enzymes results in a slight increase in absorbance at 550 nm but no decrease in absorbance at longer wavelengths over 10 h, indicating that the mutants are denaturing during the reaction. Still, these results allow us to set an upper limit on the dissociation rate constants for the

unphosphorylated enzymes of 10^{-5} s^{-1}. Upon phosphorylation, the dissociation rate constants for all three mutants increase to close to the value for wild-type TyrH (Table 3.1), establishing that the regulatory functions of the mutant enzymes are not significantly altered by the mutations.

Table 3.1 : Steady-state kinetic parameters and dopamine dissociation rate constants of F14W/F_3W TyrH, F34W/F_3W TyrH and F74W/F_3W TyrH.

Enzyme	**K_{PH4}[a] (μM)**	**K_{tyr}[b] (μM)**	**k_{cat} (min^{-1})**	**10^3 k_{off}[c] (s^{-1})**	
				unphosphorylated	**phosphorylated**
wild-type	45 ± 8	47 ± 6	138 ± 5	0.0007[d]	0.87 ± 0.02
F14W/ F_3W	55 ± 8	24 ± 4	109 ± 4	<0.01	0.38 ± 0.02
F34W/ F_3W	77 ± 7	58 ± 4	121 ± 3	<0.01	0.39 ± 0.01
F74W/ F_3W	65 ± 7	43 ± 6	104 ± 4	<0.01	0.40 ± 0.01

Conditions: [a]50 mM Hepes, pH 7, 1 mM DTT, 10 μM ferrous ammonium sulfate, 10 μg/ml catalase, 100 μM tyrosine with 5 to 400 μM 6-$MePH_4$ at 25 °C; [b]50 mM Hepes, pH 7, 1 mM DTT, 10 μM ferrous ammonium sulfate, 10 μg/ml catalase, 400 μM 6-$MePH_4$ with 5 to 400 μM tyrosine at 25 °C; [c]50 mM Hepes, pH 7, 100 mM KCl, 10% glycerol, ~30 μM enzyme, 45 μM dopamine, 30 μM DPTA, 1mM DHN at 10 °C; [d] from reference (*112*), at 15 °C.

Fluorescent quenching with acrylamide. Acrylamide quenching was used as a probe for changes in solvent accessibility of the individual tryptophan residues upon phosphorylation. The results are shown as Stern-Volmer plots in Figure 3.2. The values of the Stern-Volmer quenching constants (K_{SV}) for the mutant enzymes were determined from the slopes of the plots and are given in Table 3.2. Phosphorylation does not affect

the K_{SV} value for F74W/F_3W TyrH. In contrast, phosphorylation results in an increase of 12% in the K_{SV} value for F34W/F_3W TyrH and a smaller decrease (~5%) in the K_{SV} value for F14W/F_3W TyrH.

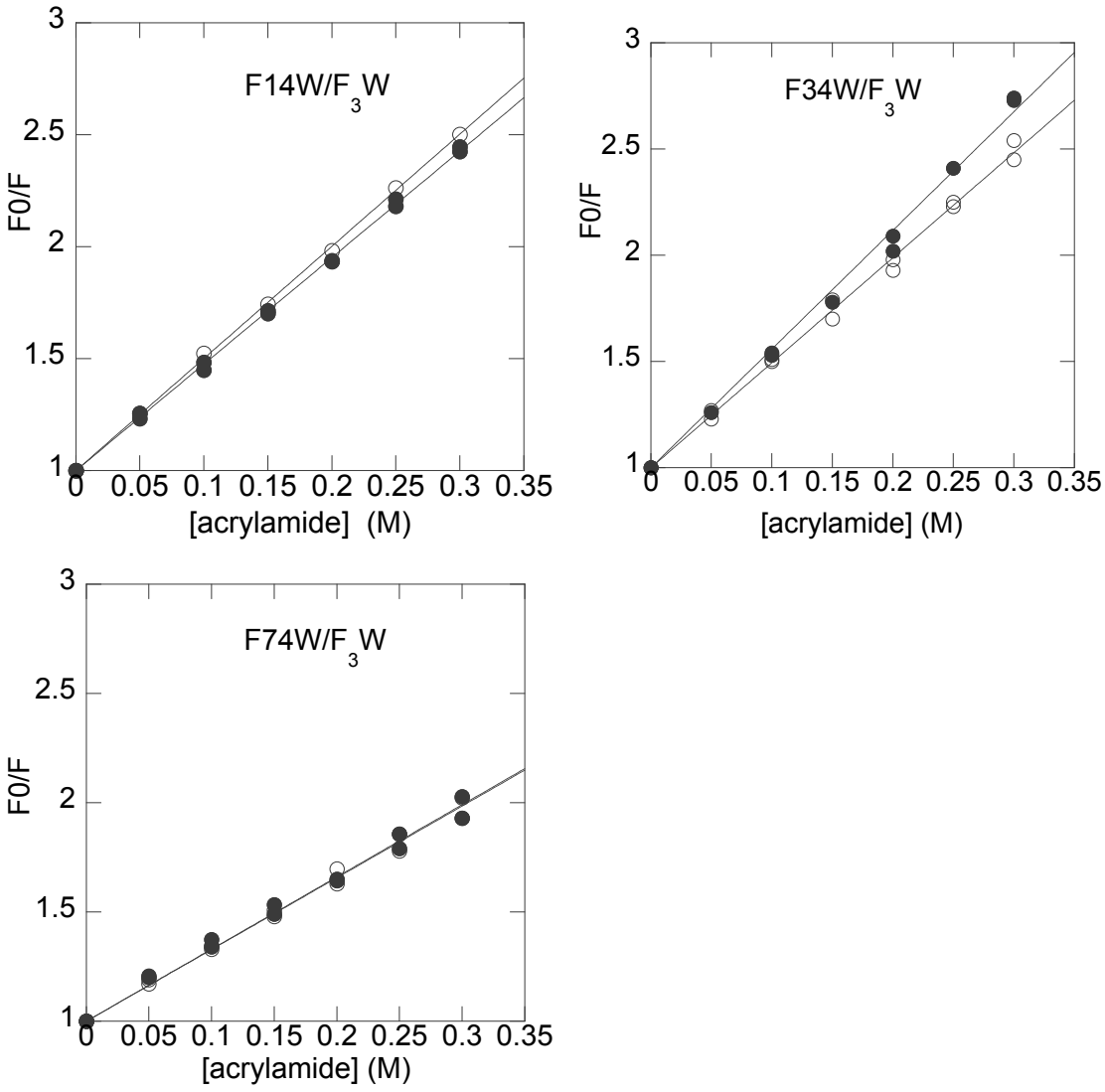

Figure 3.2: Fluorescence quenching by acrylamide of F14W/F_3W TyrH, F34W/F_3W TyrH and F74W/F_3W TyrH. Open symbols, unphosphorylated enzyme; solid symbols, phosphorylated enzyme.

Table 3.2: Effects of phosphorylation on the fluorescence parameters of F14W/F_3W TyrH, F34W/F_3W TyrH and F74W/F_3W TyrH.

enzyme	**K_{sv} (M^{-1})**	**τ (ns)**	**k_q ($M^{-1}ns^{-1}$)**	***anisotropy***	***r_0 - r_∞***	**θ_1 (ns)**
F14W/ F_3W	5.01 ± 0.03	3.26 ± 0.10	1.53 ± 0.05	0.185 ± 0.004	0.060 ± 0.008	1.27 ± 0.15
pF14W/ F_3W	4.76 ± 0.02	3.40 ± 0.02	1.40 ± 0.01	0.177 ± 0.001	0.069 ± 0.009	1.27 ± 0.15
F34W/ F_3W	4.94 ± 0.05	3.35 ± 0.09	1.47 ± 0.04	0.198 ± 0.002	0.061 ± 0.002	1.00 ± 0.09
pF34W/ F_3W	5.59 ± 0.08	3.46 ± 0.02	1.62 ± 0.02	0.168 ± 0.001	0.080 ± 0.002	1.00 ± 0.09
F74W/ F_3W	3.28 ± 0.04	2.71 ± 0.05	1.21 ± 0.02	0.234 ± 0.003	0.048 ± 0.007	1.62 ± 0.12
pF74W/ F_3W	3.30 ± 0.05	2.75 ± 0.02	1.20 ± 0.02	0.232 ± 0.004	0.036 ± 0.006	1.62 ± 0.12

The phosphorylated enzymes have a lower case p in the front of the names.

Fluorescence lifetimes. The fluorescence lifetimes of the unique tryptophan residues in each of the three mutants were determined using the multi-frequency domain method, in which phase and modulation are measured as a function of the excitation frequency. The fluorescence lifetimes (τ) were analyzed as continuous Lorentzian distributions with width W and central lifetimes C (*113-115*). F14W/F_3W TyrH and F34W/F_3W TyrH have comparable lifetimes of ~3.4 ns, while F74W/F_3W TyrH has a shorter lifetime of 2.7 ns (Table 3.2). The lifetimes of F14W/F_3W TyrH and F34W/F_3W TyrH both increased by ~ 0.1 ns upon Ser40 phosphorylation, while the lifetime of F74W/F_3W TyrH was not altered upon phosphorylation. Knowledge of the lifetimes allows the K_{sv} values in Table 3.2 to be converted to the bimolecular quenching rate constants (k_q) using Equation 3. These are listed in Table 3.2. Ser40 phosphorylation decreased the k_q value of F14W/F_3W TyrH by 8%, but increased the k_q value of F34W/F_3W TyrH by 10%. The k_q value of F74W/F_3W TyrH was not altered by Ser40 phosphorylation. In addition, it is significantly smaller than the k_q values of the other two mutant proteins.

Steady-state anisotropy. Steady-state fluorescence anisotropy was performed in order to probe the impact of phosphorylation on the local flexibility of the three positions. A decrease in the local flexibility of the peptide backbone attached to a tryptophan residue is expected to result in an increase in the anisotropy of the tryptophan. The results are summarized in Table 3.2. When only the values for the unphosphorylated proteins are considered, F74W/F_3W TyrH has a much larger anisotropy value than the other two proteins, suggesting that residue 74 is in a more rigid

local environment. Phosphorylation results in a small decrease in the anisotropy of the tryptophan at position 14, while the anisotropy at position 74 is unaffected by phosphorylation (Table 3.2). In contrast, the anisotropy at position 34 is significantly smaller in the phosphorylated enzyme. This decrease of anisotropy is consistent with an increase in the flexibility at this position upon phosphorylation.

Dynamic anisotropy. To further quantify the rotational properties of each tryptophan and the effect of phosphorylation, the dynamic anisotropy of each was determined. The phase difference and modulation ratio as a function of frequency for each protein are shown in Figure 3.3. With the exception of the data at the highest frequency used, the dynamic anisotropies of F14W/F_3W and F74W/F_3W TyrH are not affected by phosphorylation. In contrast, phosphorylation resulted in a substantial change in the dynamic anisotropy F34W/F_3W TyrH at all frequencies. These results agree with the effects of phosphorylation on the steady-state anisotropies.

The data in Figure 3.3 were analyzed using equation 3.4, which applies for a system with a global rotation plus a hindered local rotation (*116, 117*). Here, r_0 is the anisotropy at time zero and is independent of the rotational motion, r_∞ is the anisotropy persisting after a relative long time ($t >> \theta_1$), and θ_1 and θ_2 are the local and global rotational correlation times ($\theta_1 << \theta_2$). Thus, r_∞ and $r_0 - r_\infty$ are the contributions of the slow global rotation and the faster local rotation, respectively. The value of θ_2, which reflects the motion of the entire protein, was fixed at 115 ns based on our earlier study of the fluorescence properties of TyrH (*106*). The values of r_0 and θ_1 from independent analyses of the phosphorylated and unphosphorylated enzymes were similar, so a global

analysis of the data was performed for each mutant protein, combining the data for the phosphorylated and unphosphorylated forms and assigning the same r_0 and θ_1 irrespective of phosphorylation status. The analyses yielded the same r_0 value of 0.21 ± 0.01 for all three proteins, but the θ_1 and r_∞ values differed (Table 3.2). Only in the case of F34W/F_3W TyrH is there a significant increase in the value of r_0 - r_∞ upon phosphorylation (Table 3.2). However, the errors in the values of r_0 - r_∞ for F14W/F_3W TyrH and F74W/F_3W TyrH from the analyses are larger than that for F34W/F_3W TyrH; this is clearly reflected by the poorer quality of the fitting for these two proteins (Figure 3.3). The inability to fit the data may come from the limitations of describing the rotational behavior of the two mutants with only one global rotation component and one local hindered rotation component. However, using models with more local hindered rotations to fit the data did not significantly improve the fitting. Still, the raw data clearly show that Ser40 phosphorylation has a much larger effect on the dynamic anisotropy of F34W/F_3W TyrH compared to F14W/F_3W TyrH and F74W/F_3W TyrH.

$$r(t) = (r_0 - r_\infty)e^{-t/\theta 1} + r_\infty e^{-t/\theta 2} \quad (3.4)$$

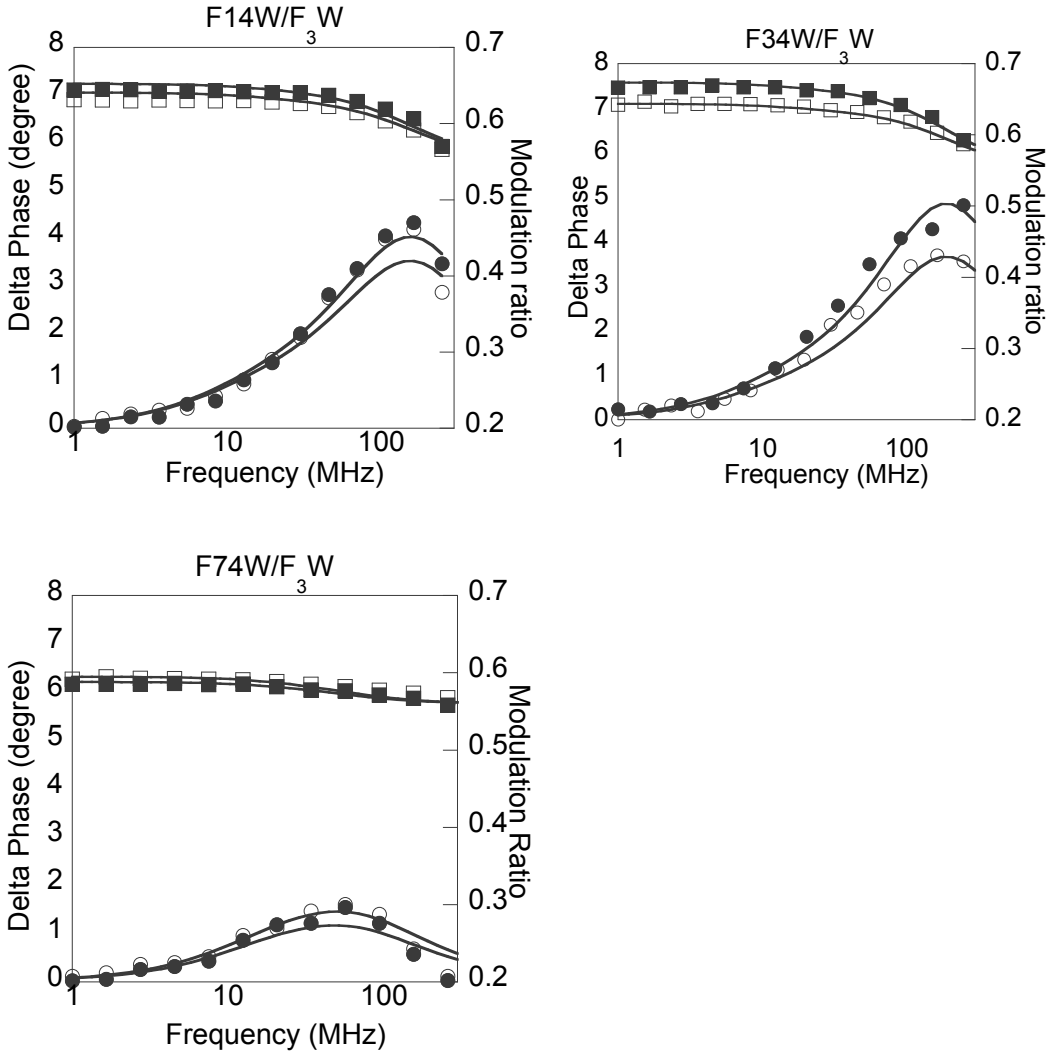

Figure 3.3: Dynamic anisotropy of F14W/F_3W TyrH, F34W/F_3W TyrH and F74W/F_3W TyrH. Open symbols, unphosphorylated enzyme; solid symbols, phosphorylated enzyme.

DISCUSSION

Previous analyses using hydrogen/deuterium exchange mass spectrometry (HDMS) established that regulation of TyrH by Ser40 phosphorylation and catecholamine binding are accompanied by structural rearrangements. Three peptides were shown to be involved in the structural changes accompanying dopamine binding (*108*). Two of the three peptides (peptide 35-41 and peptide 42-71) are in the N-terminus of the regulatory domain, while the other (peptide 295-299) is in the catalytic domain at the entrance to the active site. Upon dopamine binding all three become less accessible to solvent, consistent with the regulatory domain closing down over the active site in the dopamine-inhibited enzyme. When similar analyses were carried out with the phosphorylated enzyme, the catalytic domain peptide exhibited greater exchange, consistent with greater solvent exposure of the active site. While this provides evidence for movement of the regulatory domain away from the active site upon phosphorylation, the two peptides encompassing residues 35-71 in the regulatory domain could not be detected by mass spectrometry. The present fluorescence studies of the three single tryptophan mutants of TyrH provide insight into changes in the local dynamics of the N-terminus of the regulatory domain upon phosphorylation and substantiate the earlier model.

Similar to HDMS, which probes the solvent accessibility of amide hydrogens in peptide bonds, fluorescence quenching by acrylamide probes the accessibility of the fluorophore, tryptophan in the present case. F34W/F_3W TyrH exhibits an increase in k_q upon Ser40 phosphorylation, suggesting that Ser40 phosphorylation increases the

flexibility of the region surrounding position 34. This is confirmed by both the steady-state and dynamic anisotropy analyses. Since phosphorylation increases the lifetime of F34W/F_3W TyrH by only 0.1 ns, the change in anisotropy of F34W/F_3W TyrH upon phosphorylation can be attributed solely to a change in the rotational freedom of the indole ring. The dramatic decrease in the steady-state anisotropy upon phosphorylation of F34W/F_3W TyrH reflects an increase in the rotational motion of the side chain of the residue at position 34. The increase in the value of r_0 - r_∞ after phosphorylation of F34W/W3 TyrH can be more directly attributed to an increase in the flexibility at position 34 upon Ser40 phosphorylation. The increase in flexibility upon phosphorylation of TyrH is consistent with decreased interaction of the N-terminus of the regulatory domain with the catalytic domain.

There is a small decrease in the value of k_q for F14W/F_3W TyrH upon Ser40 phosphorylation, suggesting that this portion of the protein is more protected from solvent. In contrast, phosphorylation results in a very small decrease in the steady-state anisotropy, suggesting an increase in flexibility. There is also a small increase in the r_0 - r_∞ value upon phosphorylation, again suggesting a small increase in flexibility, but the relatively large errors in values of r_0 - r_∞ preclude drawing a definitive conclusion from the change the latter value. Overall, the data suggest that there is a small structural change in the region around residue 14 upon Ser40 phosphorylation, but it cannot be simply described as increased motion of the side chain at that position.

Peptides 28-34 and 35-41 undergo complete exchange with solvent deuterium within 7 s (*108*), indicating that the surrounding region is very flexible. The values of k_q

and r_0 - r_∞ at position 14 are comparable to those for position 34 in the unphosphorylated protein, indicating that the region around residue 14 is also very flexible. Ser19 is another phosphorylation site on the regulatory domain, and phosphorylation of TyrH at Ser19 is required for binding to 14-3-3 proteins (*75*). 14-3-3 protein binding (*118*) decreases the rate of dephosphorylation at Ser40 and Ser19 by phosphatases by decreasing the solvent accessibility of those regions (*72, 76*). Recent studies show that more than 90% of 14-3-3 binding proteins have unstructured regions (*119*), and the binding sites of 14-3-3 proteins are usually in those unstructured regions (*119*). CD analyses of the regulatory domain of TyrH indicate that ~ 45% of the regulatory domain is non-structured (*76*). Together with our results, it would be reasonable that region surrounding position 14 does not have a rigid structure so that it may bind 14-3-3 proteins.

Neither the acrylamide quenching nor the anisotropy suggest that there are significant differences in the flexibility of the residue at position 74 upon phosphorylation. Compared with F14W/F_3W TyrH and F34W/F_3W TyrH, F74W/F_3W TyrH has dramatically smaller values of k_q and r_0 - r_∞. This is consistent with position 74 being in a more rigid environment than position 14 and 34. The present results are consistent with the HDMS results, in which peptide 75-83 shows less deuterium incorporation than peptide 28-34, and neither dopamine binding nor phosphorylation alters the deuterium incorporation content into peptide 75-83. Theoretically, a less exposed fluorophore should have an increased lifetime, but the lifetime of F74W/F_3W TyrH is ~ 0.7 ns smaller than the lifetimes of the other two proteins in this study.

Lifetimes can be influenced by many factors other than solvation. Intermolecular interaction with nearby side chains groups (e.g. histidyl, carboxyl groups) tend to quench a fluorophore (*114*), resulting in a decreased lifetime. The indole ring could also be quenched from a distance by the protein-bound iron in TyrH (*114*). As a result, lifetimes are not a reliable indicator for local environment.

Both the previous HDMS data and the present fluorescence results support a regulation-driven shift between a closed conformation and an open conformation for TyrH (Figure 3.4). In this model, dopamine binding stabilizes a closed form of the enzyme in which the N-terminus of the regulatory domain covers the active site entrance, while Ser40 phosphorylation shifts the protein to an open form in which the N-terminus of the regulatory domain has moved away from the active site. Phosphorylation results in smaller differences in solvent accessibility than dopamine binding (*108*), suggesting that the resting enzyme is closer to the open form. This agrees with the observation that deletion of the regulatory domain of TyrH has little effect on the steady-state kinetic parameters (*35, 93*), indicating that the regulatory domain of the resting enzyme does not restrict substrates from accessing the active site.

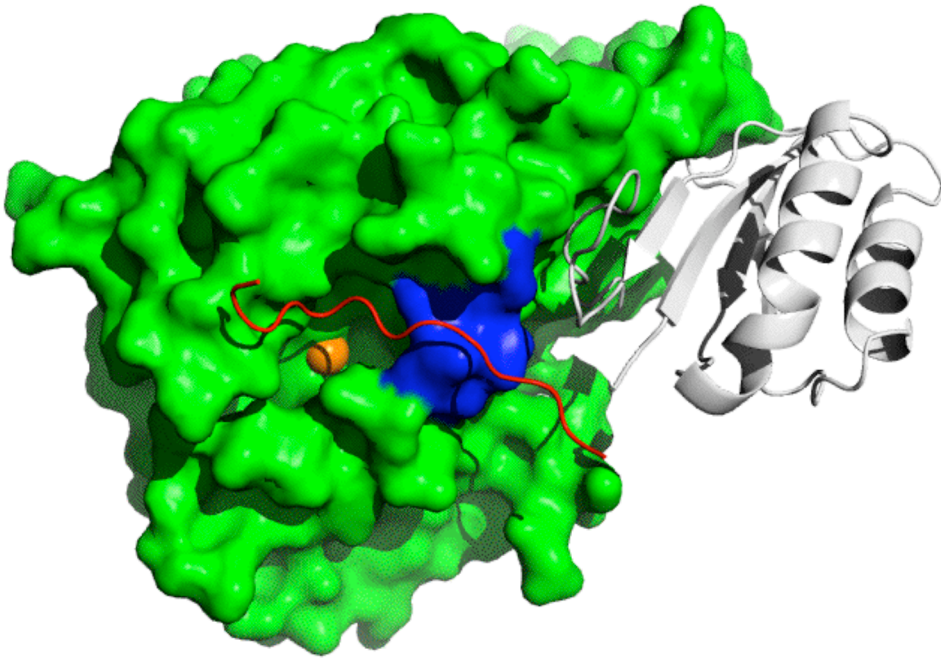

Figure 3.4. Interactions between the regulatory domain and the catalytic domain of PheH. The catalytic domain is shown as surface rendering and the regulatory domain is shown as cartoon. The active site iron is shown as an orange sphere. Residues of the N-terminus of the regulatory domain are shown in red. Residues 249-253 (295-299 in TyrH) are shown in blue. The image was generated from PDB file 2PHM.

The dissociation rate constants for catecholamines increase several hundred-fold upon phosphorylation (*78, 79*). The rate constant for dissociation of dopamine from TyrH lacking the regulatory dopamine is half of that of Ser40-phosphorylated TyrH (Wang and Fitzpatrick, unpublished data), suggesting that the restricting effect of the regulatory domain in the closed form is responsible for tight binding of catecholamines. Previous studies show that the amino group of catecholamines is critical for tight binding (*108*). Crystal structures of the catalytic domain of PheH with catecholamine show that the amino group protrudes out of the active site, lacking any interaction with the catalytic domain (*120*). These results suggest that there is a direct interaction between the regulatory domain and the amino group of catecholamines in the closed form of TyrH.

Studies of the dynamic anisotropy at position 184 of unphosphorylated TyrH have been carried out previously (*106*). Position 184 is at the center of one of the surface loops near the active site entrance and this loop has been shown to be required for catalysis (*39*). The value of $r_0 - r_\infty$ at position 184, 0.048, is comparable to the value at position 74. Residues in loops are usually more dynamic than those in the secondary structures, indicating that position 74 is in a relatively dynamic region. Compared with position 184, the significantly larger values of $r_0 - r_\infty$ for positions 34 and 14 indicate that these two positions are highly dynamic, consistent with the peptides containing these residues lacking a stable structure. Taken together, our results suggest that the entire N-terminal half of the regulatory domain is highly flexible.

In conclusion, we have used three single-tryptophan mutants of TyrH to investigate the structural effects of Ser40 phosphorylation of TyrH. The results show that the region near residue 34 has greater flexibility upon phosphorylation, while the regions near residue 14 and residue 74 do not undergo structural rearrangement upon phosphorylation. This is consistent with TyrH existing in open and closed conformations, the equilibrium between which is critical to regulation.

CHAPTER IV

IDENTIFICATION OF A DIMERIZATION DOMAIN WITHIN THE REGULATORY DOMAIN OF TYROSINE HYDROXYLASE

Tyrosine hydroxylase (TyrH) converts tyrosine into dihydroxyphenylalanine (DOPA) utilizing tetrahydrobiopterin and molecular oxygen (*5, 21, 121*). This is the first and rate-limiting step in the synthesis of catecholamine neurotransmitters. TyrH is a member of the small family of aromatic amino acid hydroxylases that also includes phenylalanine hydroxylase (PheH) and tryptophan hydroxylase (TrpH). PheH is the rate-limiting enzyme of phenylalanine catabolism and TrpH is the rate-limiting enzyme of serotonin biosynthesis. As a result, the three enzymes are related to many human diseases, such as Parkinson's disease (*122*) and phenylketonuria (*123*).

The mammalian forms of these enzymes contain regulatory domains at their N-termini and catalytic domains at their C-termini. The catalytic domains contain all the residues for catalysis (*93*), while the regulatory domains are responsible for allosteric regulation (*5*). The mammalian forms of these enzymes are homotetramers (*95, 124*), although PheH is also reported to be a mixture of tetramers and dimers (*125, 126*). The removal of the N-termini does not change the oligomerization state of the proteins (*14, 35, 127-129*), while further truncation of the C-terminal coiled coil yields monomeric proteins in solution (*24, 26, 32, 36*) or dimeric PheH in crystals (*13*). Although the sequences of the catalytic domains of the rat enzymes are ~ 50% identical, the regulatory

domains of the three enzymes are not homologous (*15, 16*), consistent with their different regulatory mechanisms (*5*).

As the rate-limiting enzyme in the catecholamine synthetic pathway, TyrH is under tight regulation (*4*). The active site of TyrH contains a non-heme iron atom that must be in the ferrous form for catalysis (*12, 80*). Molecular oxygen oxidizes ferrous TyrH to the ferric form (*80*), which has a high affinity for catecholamines (*78, 79*). The binding of a catecholamine to the ferric active site iron prevents the reduction of TyrH to the ferrous form, trapping TyrH in the ferric form (*77*). Phosphorylation of TyrH at serine 40 increases the rate constant for dissociation of catecholamines by as much as three orders of magnitude (*78, 79*). This allows the catecholamine to dissociate from the enzyme and the enzyme to be reactivated. A crystal structure is only available for the C-terminal catalytic domain of TyrH (*14*). Limited proteolysis and hydrogen deuterium exchange mass spectrometry (HDMS) have shown that the movement of the first ~ 70 residues is directly involved in regulation (*86, 108*). These residues have been proposed to function like a lid that closes the entrance to the active site after a catecholamine is bound, making the dissociation of the catecholamine extremely slow. Upon Ser40 phosphorylation, the lid opens, facilitating the exit of the catecholamine.

Residues 70 - 150 of TyrH were recently proposed to be an ACT domain (*29, 130*). ACT domains are typically involved in regulation of amino acid metabolism (*131*); binding the amino acid directly to the ACT domain can either increase or decrease the amino acid metabolism (*131*). Pre-incubation of PheH with phenylalanine activates the enzyme, and this activation can be abolished by deletion or mutation of the ACT domain

in the regulatory domain (*132-134*). However, whether there is a direct interaction between phenylalanine and the ACT domain is under debate (*123, 135, 136*). The function of this domain in TyrH has not been established. We describe here the identification of a dimerization domain within the ACT domain of TyrH.

EXPERIMENTAL PROCEDURES

Materials. Porcine stomach pepsin A was purchased from Worthington Biochemical Co. (Lakewood, NJ). Deuterium oxide (D_2O, 99% D) was purchased from Cambridge Isotope Laboratories (Andover, MA). Hepes (4-(2-hydroxyethyl)-1-1piperazineethanesulfonic acid) was purchased from USB Co. (Cleveland, OH). Tyrosine, phenylalanine and glycerol were from Sigma-Aldrich Chemical Co. (St. Louis, MO). All other materials were of the highest purity commercially available.

Protein purification. Wild-type TyrH, the N-terminal truncation mutants Δ32 TyrH and Δ68 TyrH, and the regulatory domain of TyrH were purified as previously described (*20, 33, 35*); the C-terminal deletion mutant 54k TyrH (lacking the last 20 amino acids) was purified using the same protocol as for wild-type TyrH. The purification of Δ155 TyrH (deleting the N-terminal regulatory domain) was as described previously with modifications (*35*). A Q-Sepharose column (10 × 300 mm) was used instead of a DEAE-Sepharose column; this was eluted with a linear gradient from 0 to 1 M KCl in 50 mM Hepes, 10 % glycerol. A Sephacryl S-300 gel-filtration column (20 × 600 mm) was used instead of a MonoQ column; this was eluted with 50 mM Hepes, 10 % glycerol and 100 mM KCl. To make apo-proteins, the purified wild-type TyrH or

Δ155 TyrH was dialyzed against 50 mM Hepes (pH 7.3), 10 % glycerol and 2 mM EDTA for three changes, followed by three changes of 200 mM Hepes (pH 7.3), 10 % glycerol and 100 mM KCl. The iron content of these two proteins was ≤ 5% as determined by atomic absorbance (*80*). All the other proteins contained a stoichiometric amount of ferric iron.

Hydrogen deuterium exchange mass spectrometry. Here, both wild-type TyrH and Δ155 TyrH were used to study the structural influence of tyrosine binding. A stoichiometric amount of 6 mM $Fe(NH_4)_2SO_4$ was added to 300 μM apo-protein in 200 mM Hepes (pH 7.3), 10 % glycerol and 100 mM KCl, under an argon atmosphere. To obtain tyrosine-bound protein, tyrosine was added to the protein solution to a final concentration of 400 μM. D_2O buffers with/without 400 μM tyrosine were made anaerobic by alternating vacuum and argon flushing before adding to enzyme. The rest of the experiment was performed as previously described (*108*), except that all procedures before quenching with 300 mM H_3PO_4 at 4 ^oC were under anaerobic conditions. The errors were calculated from the repeat of each condition.

Data analysis. The raw data from MS was first processed with the Thermo Finnigan Xcalibur software, and the spectrum of individual peptide was transferred to program MagTran to calculate the number of deuterium incorporation. The back exchange was corrected as previously described (*108*). The time dependent incorporation of deuterium of each peptide was fitted to Equation 1, where N is the maximum number of exchangeable amide hydrogens of the timecourse, and A and B are the numbers of amide hydrogen having exchange rate constants k_1 and k_2, respectively.

$$Y = N - Ae^{-k_1 t} - Be^{-k_2 t} \quad (4.1)$$

Gel-filtration chromatography. Apparent molecular weights were determined by chromatography on a Superdex-200 gel filtration column (16 × 600 mm or 10 × 300 mm) equilibrated with 50 mM Hepes, 100 mM KCl and 10 % glycerol at 25 ^{o}C. When the effect of tyrosine or phenylalanine was to be determined, enzyme was incubated in the same buffer for 30 min at 4 ^{o}C before being loaded onto the column. The column buffer also contained phenylalanine or tyrosine at the same concentration. The proteins used as standards were apo-ferritin, catalyse, β-amylase, aldolase, bovine serum albumin (BSA), carbonate anhydrase and ribonuclease A. Repeated chromatography of individual proteins was performed to calculate the errors.

RESULTS

Hydrogen deuterium exchange mass spectrometry (HDMS) of wild-type TyrH and Δ155 TyrH. To detect substrate-induced conformational changes of TyrH by tyrosine, we carried out an HDMS experiment using wild-type TyrH and Δ155 TyrH. Under anaerobic conditions, concentrated enzyme alone or with 400 μM tyrosine was diluted 20 fold into D_2O buffer containing the same concentration of tyrosine. Aliquots were subsequently removed and quenched with cold buffer at pH 2.4. Subsequently, the protein was proteolzed by pepsin and the peptides were separated by HPLC before detection by MS. For wild-type TyrH, the addition of tyrosine has no effect on the kinetics of deuterium incorporation into the majority of the peptides except peptide 342-348, which exhibits increased deuterium incorporation upon tyrosine binding (Figure

4.1). When Δ155 TyrH is used, in addition to peptide 342-348 (Figure 4.1), the deuterium incorporation of peptides in the entire tetramerization domain changes dramatically. The exchange pattern changes from EX2 to EX1 (Figure 4.2), and more deuterium is incorporated (Figure 4.3).

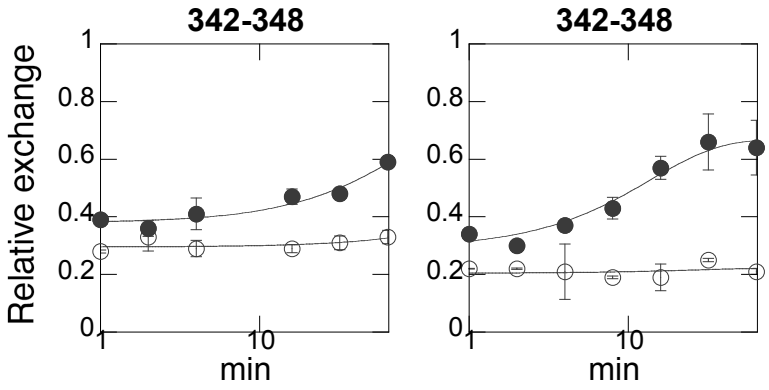

Figure 4.1: Deuterium incorporation into peptide 342-348 of wild-type TyrH (left) and Δ155 TyrH (right) in the absence (open symbols) and presence (closed symbols) of 400 μM tyrosine. Fitting data to Equation 4.1 generated the curves.

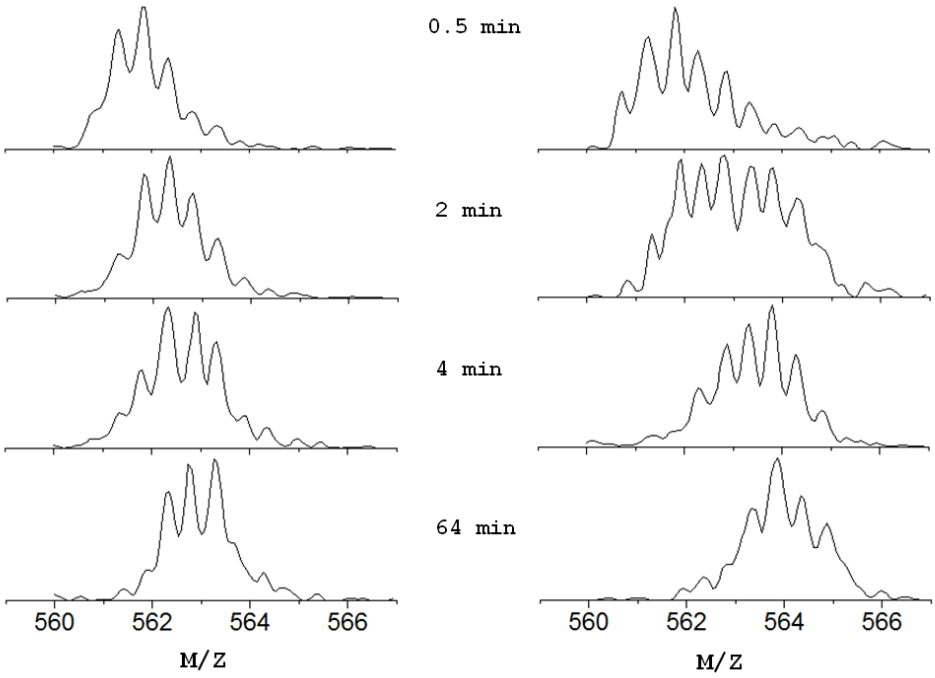

Figure 4.2: HDMS spectra of residues 488-498 of Δ155 TyrH in the absence (left) and presence (right) of 400 μM tyrosine.

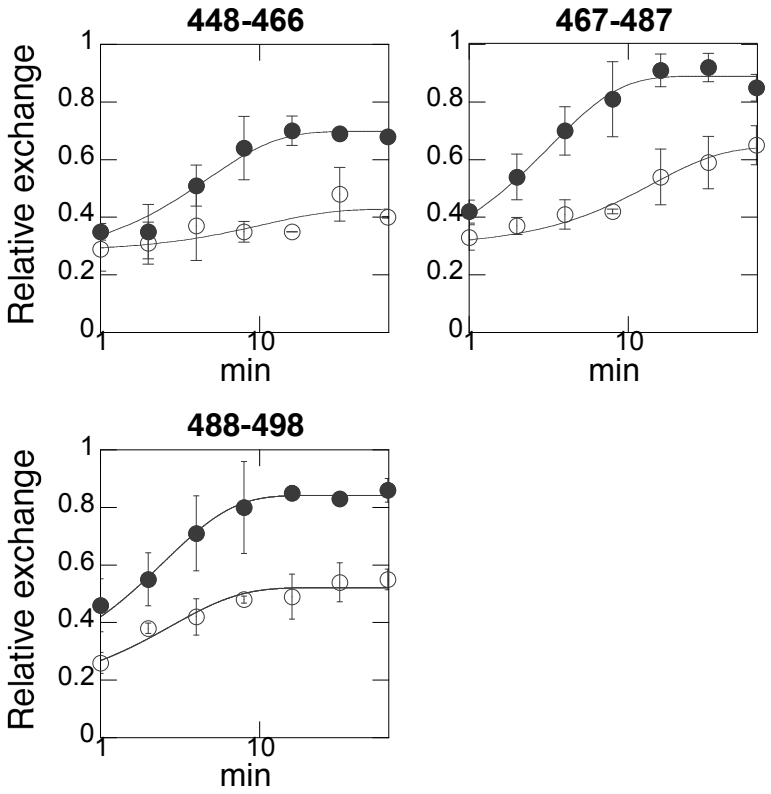

Figure 4.3: Deuterium incorporation into the tetramerization domain of Δ155 TyrH in the absence (open circles) and presence (closed circles) of 400 μM tyrosine. The exchange reaction was carried out at 25 ^{o} C in 95% D_2O (200 mM Hepes, pD 7.7) in the presence (solid symbols) or absence (open symbols) of 400 μM tyrosine. Fitting data to Equation 4.1 generated the curves.

Gel-filtration chromatography of Δ155 TyrH and wild-type TyrH. Gel-filtration chromatography was used to determine the influence of tyrosine on the quaternary structures of Δ155 TyrH and wild-type TyrH. The enzymes were incubated with or without the amino acid for 30 min at 4 ^{o}C before being loaded onto a Superdex-200 column. In the absence of tyrosine, Δ155 TyrH elutes as three major peaks with apparent molecular weights of 423 ± 12 kDa, 162 ± 5 kDa and 45 ± 3 kDa (Figure 4.4, top); a smaller peak with a molecular weight of 91 ± 5 kDa is also present (Figure 4.4, top). In presence of 500 μM tyrosine, the 162 kDa peak is much smaller and the 45 kDa peak increases dramatically (Figure 4.4, top). The molecular weights of the 162 kDa and 45 kDa species are consistent with tetramer and monomer, respectively, while the molecular weights of 420 kDa and 91 kDa could be explained by aggregated protein and a dimer. The 162 kDa and 45 kDa peaks were collected individually and concentrated. Re-chromatography of each individual peak in the presence and absence of 500 μM tyrosine reproduced the elution patterns seen in Figure 4.4 (results not shown). When different concentrations of tyrosine are used, a concentration dependent-dissociation of Δ155 TyrH is observed (Figure 4.4, top). The same dissociation effects could also be achieved by 1 mM phenylalanine, but not by alanine at concentrations up to 2 mM. A stable baseline could not be obtained using tyrosine at low protein concentration if the maximum A_{280} value of the peak was below 0.005. As a result, phenylalanine was used instead of tyrosine in those situations. When the concentration of Δ155 TyrH is lowered by about 5 fold, the protein trends to dissociate more both in the absence and in the presence of the amino acid (Figure 4.4, bottom). When the analysis is carried out with

wild-type TyrH, a major peak with a molecular weight of 246 ± 7 kDa and a very small peak with a molecular weight of 86 ± 5 kDa are seen (Figure 4.5). The presence of phenylalanine slightly increases the size of the smaller peak.

Gel-filtration chromatography of C-terminal truncation mutant. To further elucidate the contribution of the regulatory domain to the oligomerization state of TyrH, a mutant protein lacking 20 residues at the C-terminus (54k TyrH) was analyzed by gel-filtration. The k_{cat} value (37 min^{-1}) of this mutant is about 30% of wild-type TyrH and the K_m value for tyrosine (12 μM) is comparable to wild-type TyrH. For experiments with 2 - 4 μM protein injected onto the column, phenylalanine was used instead of tyrosine to take advantage of its low extinction coefficient at 280 nm. Gel-filtration chromatography of 54k TyrH at a concentration of ~ 3 μM revealed two peaks with apparent molecular weights of 132 ± 10 kDa and 85 ± 8 kDa (Figure 4.6, top), respectively; the peak with molecular weight of 132 kDa was dominant (Figure 4.6, bottom) when the initial protein concentration was increased by ~ 20-fold. An elongated shape for the monomer of 54k TyrH could account for the apparent size of 85 kDa and a dimer with two monomers side by side would have an apparent size of 132 kDa.

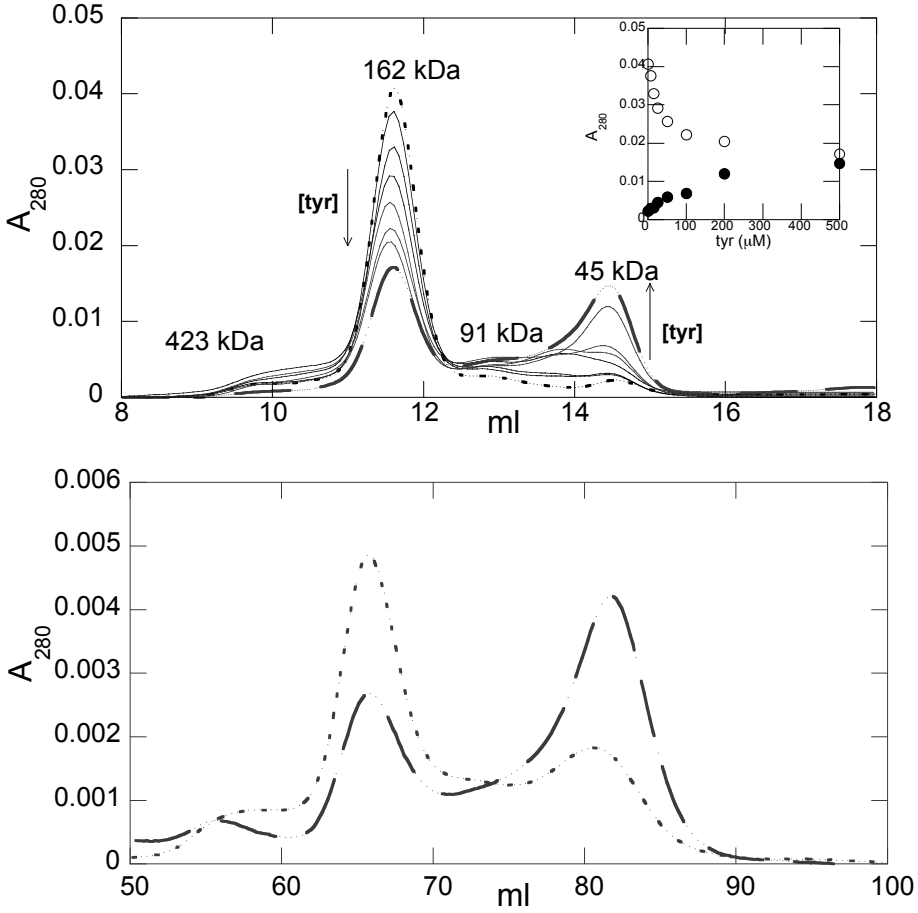

Figure 4.4: Effects of tyrosine binding on the quaternary structure of Δ155 TyrH. Top: After pre-incubation in 50 mM Hepes, 100 mM KCl, 10 % glycerol and 0, 8, 15, 25, 50, 100, 200, 500 μM tyrosine for 30 min, 100 μl of 15 μM Δ155 TyrH was injected and eluted with the same buffer in a Superdex-200 gel filtration column (10 × 300 mm). The dotted line and broken line represent the elution buffer containing 0 and 500 μM tyrosine, respectively. Inset: Maxium absorbance of tetramer (open symbols) and monomer (solid symbols) of Δ155 TyrH at each tyrosine concentration. Bottom: 500 μl of ~ 4 μM Δ155 TyrH was injected onto a Superdex-200 gel filtration column (16 × 600 mm) in the absence (dotted line) and the presence (broken line) of 1 mM phenylalanine.

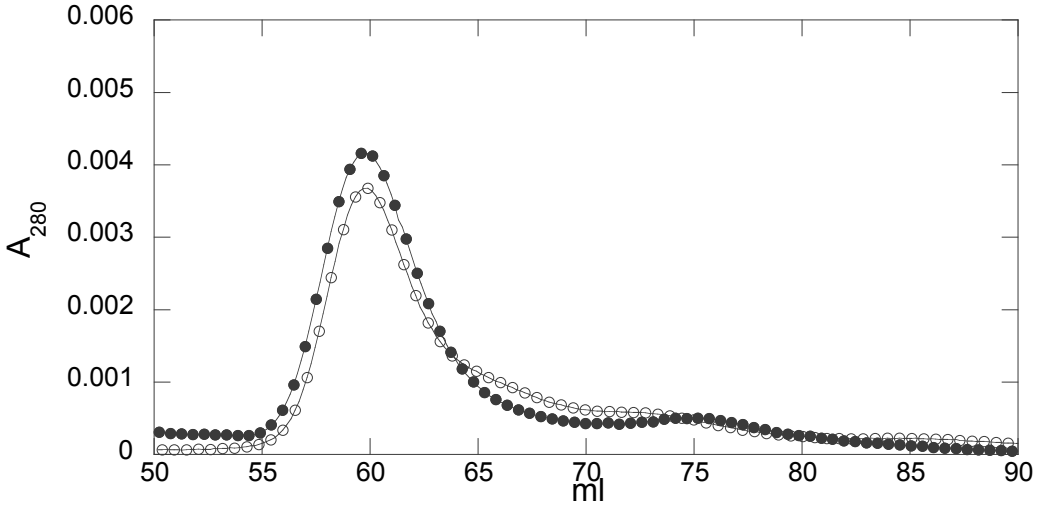

Figure 4.5: Analysis of the influence of phenylalanine on the quaternary structure of wild-type TyrH. Five hundred μl of ~ 2 μM wild-type TyrH was eluted with 50 mM Hepes, 100 mM KCl and 10 % glycerol in the absence (open symbols) and presence (solid symbols) of 1mM phenylalanine.

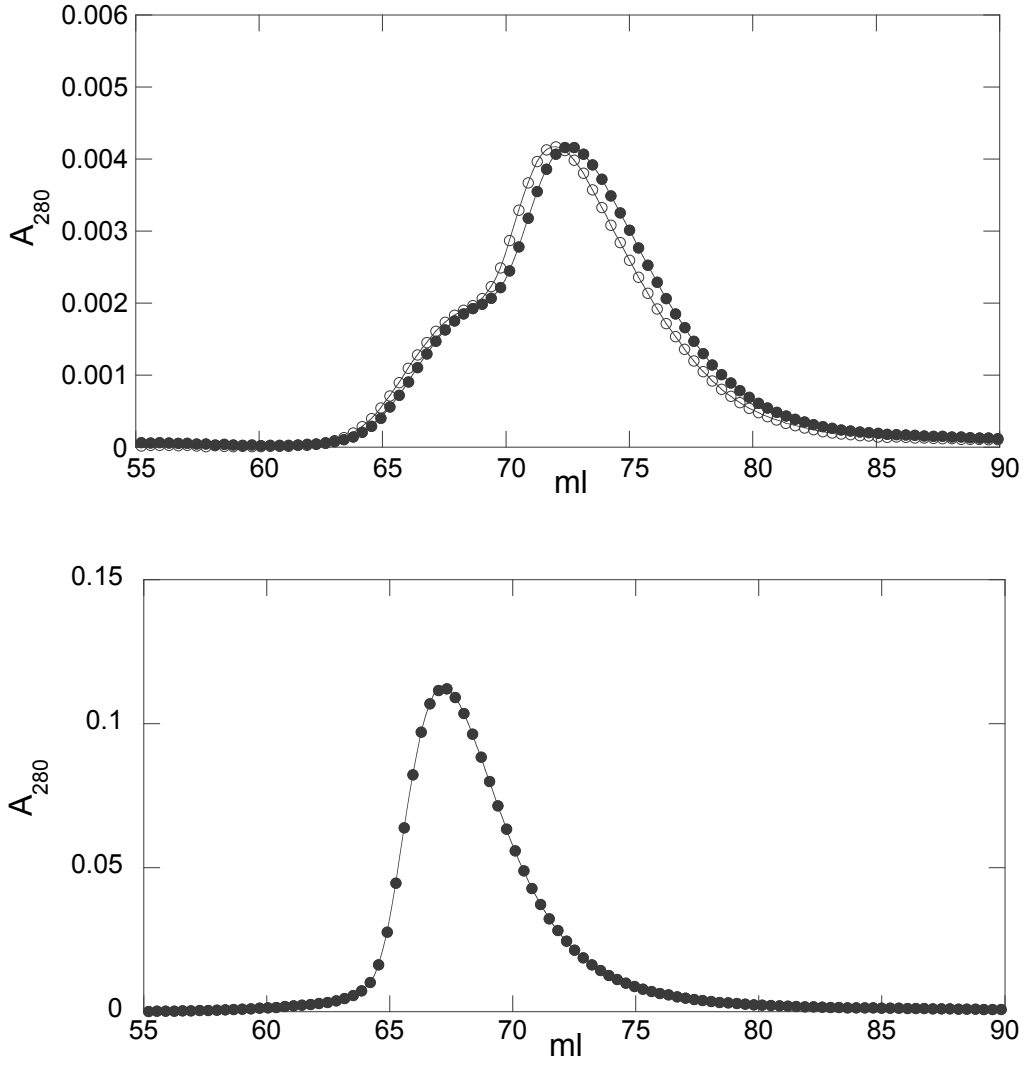

Figure 4.6: Analysis of the quaternary structure of 54k TyrH by gel-filtration. Top: Five hundred μl of ~ 3 μM 54k TyrH was eluted with 50 mM Hepes, 100 mM KCl and 10 % glycerol in the absence (open symbols) and presence (solid symbols) of 1 mM phenylalanine. For comparison, the peak of the latter is normalized to have a same maxium aborbance to the former (less than 5% difference before normalizaztion); bottom: Five hundred μl of 50 μM 54k TyrH was eluted with 50 mM Hepes, 100 mM KCl, 10 % glycerol and 1mM phenylalanine.

Gel-filtration chromatography of N-terminal truncation mutants. To further locate the dimerization domain on the regulatory domain, two mutant proteins lacking the N-terminal 32 or 68 residues, Δ32 TyrH and Δ68 TyrH, were analyzed. Gel-filtration chromatography of Δ32 TyrH revealed a major peak with a molecular weight of 223 ± 4 kDa and a very small peak with a molecular weight of 65 ± 3 kDa. The presence of 1 mM phenylalanine slightly increases the size of the smaller peak (Figure 4.7), like wild-type TyrH. A similar experiment with Δ68 TyrH showed a major peak with a molecular weight of 198 ± 6 kDa and a smaller peak with a molecular weight of 58 ± 8 kDa (Figure 4.7); the smaller peak increased in altitude in the presence of 1 mM phenylalanine (Figure 4.7), although it is still a small peak. The major peaks of Δ32 TyrH and Δ68 TyrH are consistent with tetramers; the smaller peaks represent monomers with elongated shapes.

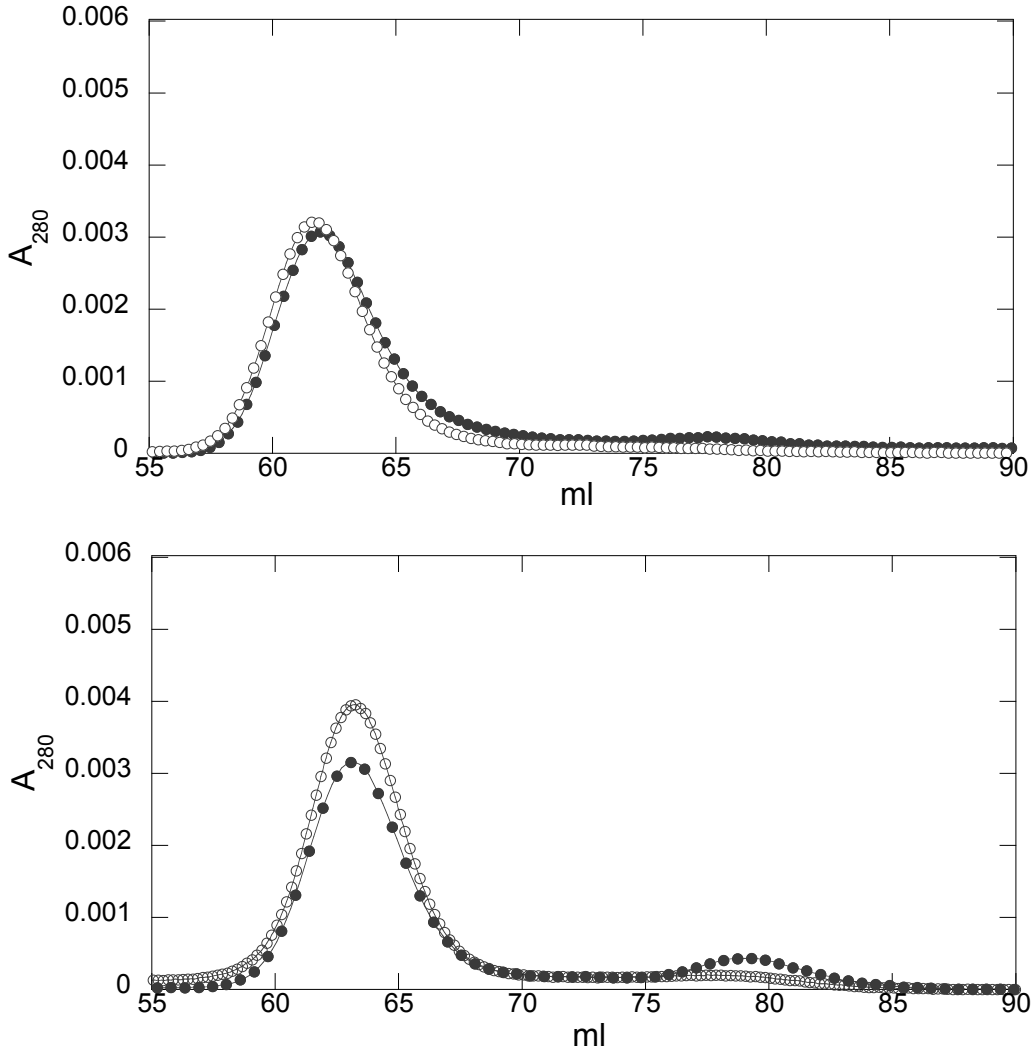

Figure 4.7: Analysis of the influence of phenylalanine on the quaternary structures of Δ32 TyrH and Δ68 TyrH by gel-filtration. Five hundred μl of ~ 2 μM Δ32 TyrH (top) or Δ68 TyrH (bottom) was loaded onto a Sephadex-200 gel filtration column (16 × 600 mm) and eluted with 50 mM Hepes, 100 mM KCl and 10 % glycerol in the absence (open symbols) or presence (solid symbols) of 1 mM phenylalanine.

DISCUSSION

The regulatory domain of TyrH is required for the modulation of enzyme activity, e.g, feedback inhibition by catecholamines or activation by phosphorylation (*5*). Phosphorylation on serine residues of the regulatory domain has also been related to protein stability (*137*). But modulation either of enzyme activity or stability is related to only the first 70 residues, and the function of residues 70-155 of the regulatory domain in TyrH is unclear. In this paper, we report a new function of residues 70-155 of the regulatory domain, dimerization.

The increase of deuterium incorporation into the tetramerization domain of Δ155 TyrH in the presence of tyrosine indicates an increase in flexibility in this region upon tyrosine binding. The EX1 exchange pattern is usually seen in studies of unfolding where a high concentration of denaturant is present and the refolding rate constant is much smaller than the exchange rate constant of the unfolded peptide (*138*). In the present case, the EX1 kinetics suggests dissociation of the tetramer. This is confirmed by the gel-filtration chromatography, in which Δ155 TyrH dissociates into monomers upon tyrosine binding. The dissociation seen in gel-filtration chromatography indicates that the refolding/re-association of the tetramerization domain is a slow process; otherwise, a clear monomer peak would not be present in the gel-filtration profile. The re-chromatography of the collected monomer peak reproduced the gel-filtration profile both in the presence and in the absence of tyrosine, indicating the dissociation is reversible and not due to the protein damage during the chromatography process.

In contrast to Δ155 TyrH, wild-type TyrH only slightly dissociates in the presence of phenylalanine when the protein concentration is very low (Figure 4.5), suggesting the existence of an inter-subunit binding region on the regulatory domain. This is supported by the results of a previous study, in which TyrH became a monomer after deletion of both the regulatory domain and C-terminal 20 amino acids (*20*), suggesting that there is no strong interaction between adjacent catalytic domains. The dimeric form of 54k TyrH is consistent with the existence of a dimerization region in the regulatory domain.

The first ~70 amino acids were recently shown to be involved in the regulation of TyrH (*86, 108*). It is not likely that the dimerization site is before residue 70, because these residues have high mobility and lack secondary structure (*108*). Consistent with this, both Δ32 TyrH and Δ68 TyrH have a very small fraction of the tetramer dissociate into monomer upon phenylalanine binding. This suggests that the main interactions required for dimerization is between residues 68 and 155, and there is a minor contribution before residue 68. Residues after 70 form an ACT domain, the function of which is unknown in TyrH. ACT domains are generally the regulatory domains of amino acid metabolizing enzymes, whose activity is modulated by the binding of amino acid to the ACT domain (*130, 131*). The regulatory domain of PheH also contains an ACT domain (*28*) that comprises the majority part of the regulatory domain. Although TyrH and PheH share a low sequence similarity before the ACT domains (residues 1-24 of PheH and 1-70 of TyrH), they share ~ 50% sequence similarity of the ACT domain and > 70% sequence identity in the catalytic domain. With no structure of the regulatory

domain of TyrH available, the structure of PheH (residues 25-452) could reflect that of TyrH (residues 71 – 498). The structure of PheH containing residues 25-452 is obtained by the alignment of the structures of two truncated PheH (one missing the first 117 residues and the other missing the last 25 residues). As shown in Figure 4.8, the ACT domains of neighboring subunits interact with both catalytic domains to form a dimer. This suggests that the ACT domains help maintain the tertiary structure of TyrH.

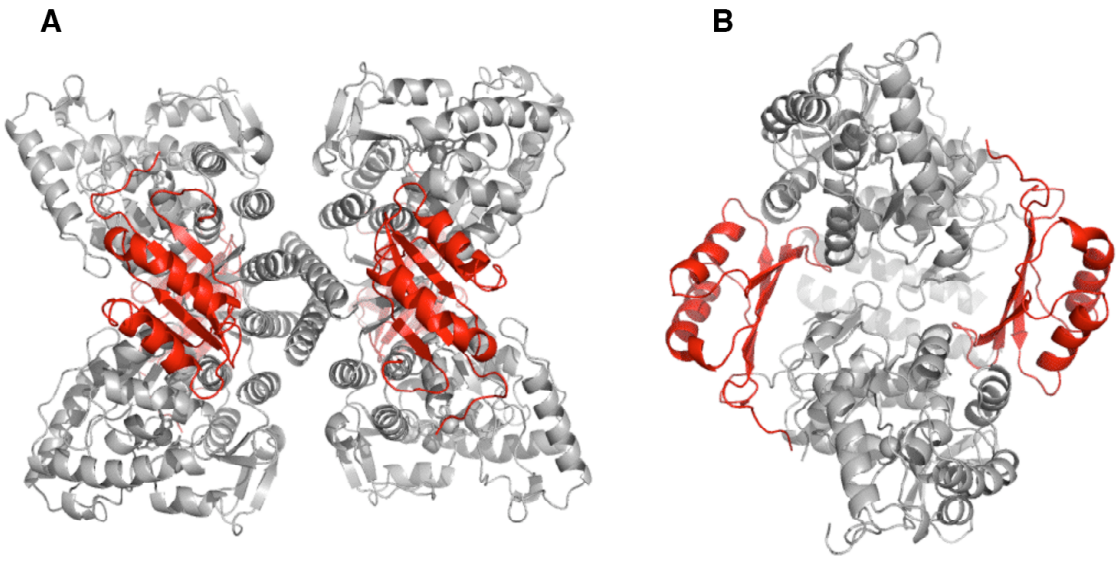

Figure 4.8: The structure of PheH. The structure is obtained by aligning the structure of PheH lacking first 117 residues (2PHM) and the structure of PheH lacking the last 25 residues (2PAH), followed by deleting the overlapping residues in 2PHM and residues before position 25 in 2PAH. The regulatory domain is in red and the rest of the molecule in gray. A: The tetrameric form of PheH shows that each regulatory domain is in contact with two catalytic domains. B: Side view of the interaction between the regulatory domain and the catalytic domain. Only two neighboring subunits are shown in B.

The small peak between the tetramer and monomer peaks seen in the gel filtration analysis of Δ155 TyrH suggests the dimer is not stable, with a strong tendency to dissociate into monomers. That the tetramer of wild-type TyrH is formed by two intermediate dimers was proposed in previously publication (*27*), based on the finding that mutations disrupting the tetramerization domain yielded mostly dimer, but very little monomer (*27*). The crystal structure of the catalytic domain of TyrH shows that the C-terminal end of the catalytic domain contains an interaction between β-sheets of two adjacent subunits (14), suggesting that the tetramer is formed by dimerization of two dimers. The β-turn interaction is not strong enough to hold a dimer, because truncating the N-terminal regulatory domain and the C-terminal tetramerization domain (but still contains the β-turns) yields a monomer, rather than a dimer (*26*). Thus, the ACT domain is responsible for keeping the intermediate dimers from dissociation. The absence of a dimer of wild-type TyrH in gel-filtration chromatography suggests that the dimer of wild-type TyrH exist only as an intermediate, which associates back to tetramer very promptly. Further, because of the reinforcement of the dimerization between the regulatory domain and the catalytic domain, the presence of tyrosine has minimal impact on the tertiary structure of wild-type TyrH.

The binding of substrates for TyrH is sequential, with pterin binding first, followed by molecular oxygen and then tyrosine (*41*), suggesting that tyrosine does not bind to TyrH productively in the absence of the other two substrates. However, there is an increase in deuterium incorporation in peptide 342-348 upon tyrosine binding in wild-type TyrH and Δ155 TyrH, suggesting that a second binding site of tyrosine rather than

the active site might be present and responsible the dissociation of Δ155 TyrH upon tyrosine binding. Consistent with this, residues 342-348 is part of a helix far away from the active site of TyrH and none of those residues have been shown to be critical for TyrH activity.

In summary, we designate another function to the regulatory domain of TyrH, which is dimerization to the catalytic domain of another subunit. We also locate this dimerization region to residues 68 - 155 by deletion mutants. This dimerization may help the protein to be more stable.

CHAPTER V

SUMMARY

This study is aiming at identifying the structural changes related to regulation of TyrH. TyrH catalyzes the hydroxylation of tyrosine into DOPA, the first and rate-limiting step in the catecholamine biosynthetic pathway. TyrH is regulated by inhibition through catecholamine binding or activation through Ser40 phosphorylation. The inhibition by catecholamines is via tight binding of catecholamines with ferric protein, while Ser40 phosphorylation activates the enzyme by facilitating catecholamines to dissociate. Structural changes related to regulation of TyrH have been suggested, but not located to specific regions.

To locate the structural changes related to regulation, hydrogen deuterium exchange mass spectrometry (HDMS) was performed. Ser40 surrounding region (residues 35-71) is identified as involved in the structural changes upon dopamine binding, although this region is not identified after Ser40 phosphorylation. In addition, a small peptide of the catalytic domain, 295-299, is also identified as involved in structural changes upon regulation. Residues 35-71 and 295-299 show less deuterium incorporation upon dopamine binding, whereas residues 295-299 have a slight increase in deuterium incorporation upon Ser40 phosphorylation. Although peptide 35-71 is lost in HDMS after Ser40 phosphorylation, results of limited proteolysis have showed that residues 33-50 become more solvent accessible upon phosphorylation. Thus, same peptides are involved in structural changes upon dopamine binding and Ser40

phosphorylation, and they undergo opposed structural changes in the two regulatory mechanisms. Peptide 295-299 is part of a loop (288-298) at the active site entrance; the other half of the loop, peptide 287-294, does not show difference in deuterium incorporation upon regulation. This suggests that the changes in deuterium incorporation of residues 295-299 upon regulation is not due to the movement of the loop, which would have lead to similar changes in deuterium incorporation in residues 287-294. Rather, it is likely that the primary conformational changes happen in peptide 35-71 upon regulation, which then causes the differences in solvent accessibility to peptide 295-299.

To further investigate the role of the regulatory domain in regulation of TyrH, acrylamide fluorescent quenching and fluorescent anisotropy were performed on mutants of TyrH containing a single tryptophan at positions 14, 34 or 74. Compared with limited-proteolysis, acrylamide fluorescent quenching could provide information on solvent accessibility more quantitatively, which would complement the missing of peptide 35-71 upon phosphorylation in HDMS. There is an increase in the solvent accessibility at position 34 upon Ser40 phosphorylation, whereas the differences in solvent accessibility at position 14 and 74 are smaller. Consistent with acrylamide fluorescent quenching, there is a decrease in steady-state anisotropy and an increase in dynamic anisotropy at position 34 upon Ser40 phosphorylation. The increase in dynamic anisotropy directly show that phosphorylation increases the flexibility of position 34 containing peptide, agreeing with that the primary movement of this region is part of the conformational changes during regulation.

Because the structure of the regulatory domain of TyrH is not available, the structure of the regulatory domain of PheH is used to explain the conformational changes of TyrH upon regulation, which shifts the equilibrium between a closed conformation and an open conformation. Upon a catecholamine binding, the N-terminus of the regulatory domain covers over the active site and interacts with peptide 295-299, shifting the equilibrium to the closed form. This prevents the dissociation of the catecholamine from the active site, making the dissociation rate constant ~ 1nM. The closed conformation also causes the N-terminus of the regulatory domain and peptide 295-299 less solvent accessible, making TyrH less susceptible to proteolysis or Ser40 phosphorylation. Upon Ser40 phosphorylation, the N-terminus of the regulatory domain moves away from the active site and peptide 295-299, shifting the equilibrium toward an open form. In the open form, the bound catecholamine could dissociate much easier, increasing the dissociation rate constant of a catecholamine to ~ 1 μM. Because the N-terminus of the regulatory domain is away from residues 295-299 in the open form, both of the N-terminus and peptide 295-299 gain more solvent accessibility. The deletion of the regulatory domain yields an enzyme with similar steady-state kinetic parameters to the resting enzyme, indicating the regulatory domain does not restrict the substrate from entering the active site. Thus the resting enzyme is more close to the open form, which is also suggested by the small increase in solvent accessibility to peptide 295-299 upon Ser40 phosphorylation.

REFERENCES

1. Alderazi, Y., Yeh, M. W., Robinson, B. G., Benn, D. E., Sywak, M. S., Learoyd, D. L., Delbridge, L. W., and Sidhu, S. B. (2005) Phaeochromocytoma: current concepts, *Med J Aust 183*, 201-204.
2. Lew, M. (2007) Overview of Parkinson's disease, *Pharmacotherapy 27*, 155S-160S.
3. Gordon, N. (2008) Segawa's disease: dopa-responsive dystonia, *Int J Clin Pract 62*, 943-946.
4. Kaufman, S. (1995) Tyrosine hydroxylase, *Adv Enzymol Relat Areas Mol Biol 70*, 103-220.
5. Fitzpatrick, P. F. (1999) Tetrahydropterin-dependent amino acid hydroxylases, *Annu Rev Biochem 68*, 355-381.
6. Molinoff, P. B., and Axelrod, J. (1971) Biochemistry of catecholamines, *Annu Rev Biochem 40*, 465-500.
7. Axelrod, J., and Daly, J. (1968) Phenol-O-methyltransferase, *Biochim Biophys Acta 159*, 472-478.
8. Blaschko, H., Richter, D., and Schlossmann, H. (1937) The oxidation of adrenaline and other amines, *Biochem J 31*, 2187-2196.
9. Eisensmith, R. C., and Woo, S. L. (1991) Phenylketonuria and the phenylalanine hydroxylase gene, *Mol Biol Med 8*, 3-18.

10. Lovenberg, W., Jequier, E., and Sjoerdsma, A. (1967) Tryptophan hydroxylation: measurement in pineal gland, brainstem, and carcinoid tumor, *Science 155*, 217-219.

11. Lucki, I. (1998) The spectrum of behaviors influenced by serotonin, *Biol Psychiatry 44*, 151-162.

12. Fitzpatrick, P. F. (1989) The metal requirement of rat tyrosine hydroxylase, *Biochem Biophys Res Commun 161*, 211-215.

13. Erlandsen, H., Fusetti, F., Martinez, A., Hough, E., Flatmark, T., and Stevens, R. C. (1997) Crystal structure of the catalytic domain of human phenylalanine hydroxylase reveals the structural basis for phenylketonuria, *Nat Struct Biol 4*, 995-1000.

14. Goodwill, K. E., Sabatier, C., Marks, C., Raag, R., Fitzpatrick, P. F., and Stevens, R. C. (1997) Crystal structure of tyrosine hydroxylase at 2.3 A and its implications for inherited neurodegenerative diseases, *Nat Struct Biol 4*, 578-585.

15. Grenett, H. E., Ledley, F. D., Reed, L. L., and Woo, S. L. (1987) Full-length cDNA for rabbit tryptophan hydroxylase: functional domains and evolution of aromatic amino acid hydroxylases, *Proc Natl Acad Sci U S A 84*, 5530-5534.

16. Abate, C., and Joh, T. H. (1991) Limited proteolysis of rat brain tyrosine hydroxylase defines an N-terminal region required for regulation of cofactor binding and directing substrate specificity, *J Mol Neurosci 2*, 203-215.

17. Daubner, S. C., Hillas, P. J., and Fitzpatrick, P. F. (1997) Expression and characterization of the catalytic domain of human phenylalanine hydroxylase, *Arch Biochem Biophys 348*, 295-302.

18. Iwaki, M., Phillips, R. S., and Kaufman, S. (1986) Proteolytic modification of the amino-terminal and carboxyl-terminal regions of rat hepatic phenylalanine hydroxylase, *J Biol Chem 261*, 2051-2056.

19. Yang, X. J., and Kaufman, S. (1994) High-level expression and deletion mutagenesis of human tryptophan hydroxylase, *Proc Natl Acad Sci U S A 91*, 6659-6663.

20. Daubner, S. C., and Piper, M. M. (1995) Deletion mutants of tyrosine hydroxylase identify a region critical for heparin binding, *Protein Sci 4*, 538-541.

21. Fitzpatrick, P. F. (2003) Mechanism of aromatic amino acid hydroxylation, *Biochemistry 42*, 14083-14091.

22. Wang, L., Erlandsen, H., Haavik, J., Knappskog, P. M., and Stevens, R. C. (2002) Three-dimensional structure of human tryptophan hydroxylase and its implications for the biosynthesis of the neurotransmitters serotonin and melatonin, *Biochemistry 41*, 12569-12574.

23. Ramsey, A. J., Daubner, S. C., Ehrlich, J. I., and Fitzpatrick, P. F. (1995) Identification of iron ligands in tyrosine hydroxylase by mutagenesis of conserved histidinyl residues, *Protein Sci 4*, 2082-2086.

24. Gibbs, B. S., Wojchowski, D., and Benkovic, S. J. (1993) Expression of rat liver phenylalanine hydroxylase in insect cells and site-directed mutagenesis of putative non-heme iron-binding sites, *J Biol Chem 268*, 8046-8052.

25. Costas, M., Mehn, M. P., Jensen, M. P., and Que, L., Jr. (2004) Dioxygen activation at mononuclear nonheme iron active sites: enzymes, models, and intermediates, *Chem Rev 104*, 939-986.

26. Lohse, D. L., and Fitzpatrick, P. F. (1993) Identification of the intersubunit binding region in rat tyrosine hydroxylase, *Biochem Biophys Res Commun 197*, 1543-1548.

27. Vrana, K. E., Walker, S. J., Rucker, P., and Liu, X. (1994) A carboxyl terminal leucine zipper is required for tyrosine hydroxylase tetramer formation, *J Neurochem 63*, 2014-2020.

28. Kobe, B., Jennings, I. G., House, C. M., Michell, B. J., Goodwill, K. E., Santarsiero, B. D., Stevens, R. C., Cotton, R. G., and Kemp, B. E. (1999) Structural basis of autoregulation of phenylalanine hydroxylase, *Nat Struct Biol 6*, 442-448.

29. Chipman, D. M., and Shaanan, B. (2001) The ACT domain family, *Curr Opin Struct Biol 11*, 694-700.

30. Andersen, O. A., Stokka, A. J., Flatmark, T., and Hough, E. (2003) 2.0A resolution crystal structures of the ternary complexes of human phenylalanine hydroxylase catalytic domain with tetrahydrobiopterin and 3-(2-thienyl)-L-

alanine or L-norleucine: substrate specificity and molecular motions related to substrate binding, *J Mol Biol 333*, 747-757.

31. Kaufman, S., and Mason, K. (1982) Specificity of amino acids as activators and substrates for phenylalanine hydroxylase, *J Biol Chem 257*, 14667-14678.

32. Dickson, P. W., Jennings, I. G., and Cotton, R. G. (1994) Delineation of the catalytic core of phenylalanine hydroxylase and identification of glutamate 286 as a critical residue for pterin function, *J Biol Chem 269*, 20369-20375.

33. Daubner, S. C., and Fitzpatrick, P. F. (1999) Site-directed mutants of charged residues in the active site of tyrosine hydroxylase, *Biochemistry 38*, 4448-4454.

34. Ellis, H. R., Daubner, S. C., McCulloch, R. I., and Fitzpatrick, P. F. (1999) Phenylalanine residues in the active site of tyrosine hydroxylase: mutagenesis of Phe300 and Phe309 to alanine and metal ion-catalyzed hydroxylation of Phe300, *Biochemistry 38*, 10909-10914.

35. Daubner, S. C., Lohse, D. L., and Fitzpatrick, P. F. (1993) Expression and characterization of catalytic and regulatory domains of rat tyrosine hydroxylase, *Protein Sci 2*, 1452-1460.

36. Moran, G. R., Daubner, S. C., and Fitzpatrick, P. F. (1998) Expression and characterization of the catalytic core of tryptophan hydroxylase, *J Biol Chem 273*, 12259-12266.

37. McKinney, J., Teigen, K., Froystein, N. A., Salaun, C., Knappskog, P. M., Haavik, J., and Martinez, A. (2001) Conformation of the substrate and pterin

cofactor bound to human tryptophan hydroxylase. Important role of Phe313 in substrate specificity, *Biochemistry 40*, 15591-15601.

38. Daubner, S. C., Moran, G. R., and Fitzpatrick, P. F. (2002) Role of tryptophan hydroxylase phe313 in determining substrate specificity, *Biochem Biophys Res Commun 292*, 639-641.

39. Daubner, S. C., McGinnis, J. T., Gardner, M., Kroboth, S. L., Morris, A. R., and Fitzpatrick, P. F. (2006) A flexible loop in tyrosine hydroxylase controls coupling of amino acid hydroxylation to tetrahydropterin oxidation, *J Mol Biol 359*, 299-307.

40. Daubner, S. C., Melendez, J., and Fitzpatrick, P. F. (2000) Reversing the substrate specificities of phenylalanine and tyrosine hydroxylase: aspartate 425 of tyrosine hydroxylase is essential for L-DOPA formation, *Biochemistry 39*, 9652-9661.

41. Fitzpatrick, P. F. (1991) Steady-state kinetic mechanism of rat tyrosine hydroxylase, *Biochemistry 30*, 3658-3662.

42. Dix, T. A., Bollag, G. E., Domanico, P. L., and Benkovic, S. J. (1985) Phenylalanine hydroxylase: absolute configuration and source of oxygen of the 4a-hydroxytetrahydropterin species, *Biochemistry 24*, 2955-2958.

43. Davis, M. D., and Kaufman, S. (1989) Evidence for the formation of the 4a-carbinolamine during the tyrosine-dependent oxidation of tetrahydrobiopterin by rat liver phenylalanine hydroxylase, *J Biol Chem 264*, 8585-8596.

44. Francisco, W. A., Tian, G., Fitzpatrick, P. F., and Klinman, J. P. (1998) Oxygen-18 kinetic isotope effect studies of the tyrosine hydroxylase reaction: evidence of rate limiting oxygen activation, *Biochemistry 120*, 4057-4062.

45. Ellis, H. R., Daubner, S. C., and Fitzpatrick, P. F. (2000) Mutation of serine 395 of tyrosine hydroxylase decouples oxygen-oxygen bond cleavage and tyrosine hydroxylation, *Biochemistry 39*, 4174-4181.

46. Wasinger, E. C., Mitic, N., Hedman, B., Caradonna, J., Solomon, E. I., and Hodgson, K. O. (2002) X-ray absorption spectroscopic investigation of the resting ferrous and cosubstrate-bound active sites of phenylalanine hydroxylase, *Biochemistry 41*, 6211-6217.

47. Andersen, O. A., Flatmark, T., and Hough, E. (2002) Crystal structure of the ternary complex of the catalytic domain of human phenylalanine hydroxylase with tetrahydrobiopterin and 3-(2-thienyl)-L-alanine, and its implications for the mechanism of catalysis and substrate activation, *J Mol Biol 320*, 1095-1108.

48. Meyer-Klaucke, W., Winkler, H., Schunemann, V., Trautwein, A. X., Nolting, H. F., and Haavik, J. (1996) Mossbauer, electron-paramagnetic-resonance and X-ray-absorption fine-structure studies of the iron environment in recombinant human tyrosine hydroxylase, *Eur J Biochem 241*, 432-439.

49. Chow, M. S., Eser, B. E., Wilson, S. A., Hodgson, K. O., Hedman, B., Fitzpatrick, P. F., and Solomon, E. I. (2009) Spectroscopy and kinetics of wild-type and mutant tyrosine hydroxylase: mechanistic insight into O2 activation, *J Am Chem Soc 131*, 7685-7698.

50. Solomon, E. I., Brunold, T. C., Davis, M. I., Kemsley, J. N., Lee, S. K., Lehnert, N., Neese, F., Skulan, A. J., Yang, Y. S., and Zhou, J. (2000) Geometric and electronic structure/function correlations in non-heme iron enzymes, *Chem Rev 100*, 235-350.

51. Solomon, E. I. (2001) Invited award contribution for ACS Award in Inorganic Chemistry. Geometric and electronic structure contributions to function in bioinorganic chemistry: active sites in non-heme iron enzymes, *Inorg Chem 40*, 3656-3669.

52. Neidig, M. L., and Solomon, E. I. (2005) Structure-function correlations in oxygen activating non-heme iron enzymes, *Chem Commun (Camb)*, 5843-5863.

53. Pavon, J. A., and Fitzpatrick, P. F. (2009) Demonstration of a peroxide shunt in the tetrahydropterin-dependent aromatic amino acid monooxygenases, *J Am Chem Soc 131*, 4582-4583.

54. Eser, B. E., Barr, E. W., Frantom, P. A., Saleh, L., Bollinger, J. M., Jr., Krebs, C., and Fitzpatrick, P. F. (2007) Direct spectroscopic evidence for a high-spin Fe(IV) intermediate in tyrosine hydroxylase, *J Am Chem Soc 129*, 11334-11335.

55. Fitzpatrick, P. F. (1991) Studies of the rate-limiting step in the tyrosine hydroxylase reaction: alternate substrates, solvent isotope effects, and transition-state analogues, *Biochemistry 30*, 6386-6391.

56. Pavon, J. A., and Fitzpatrick, P. F. (2006) Insights into the catalytic mechanisms of phenylalanine and tryptophan hydroxylase from kinetic isotope effects on aromatic hydroxylation, *Biochemistry 45*, 11030-11037.

57. Panay, A. J., and Fitzpatrick, P. F. (2008) Kinetic isotope effects on aromatic and benzylic hydroxylation by chromobacterium violaceum phenylalanine hydroxylase as probes of chemical mechanism and reactivity, *Biochemistry 47*, 11118-11124.

58. Hillas, P. J., and Fitzpatrick, P. F. (1996) A mechanism for hydroxylation by tyrosine hydroxylase based on partitioning of substituted phenylalanines, *Biochemistry 35*, 6969-6975.

59. Guroff, G., Levitt, M., Daly, J., and Udenfriend, S. (1966) The production of meta-tritiotyrosine from p-tritiophenylalanine by phenylalanine hydroxylase, *Biochem Biophys Res Commun 25*, 253-259.

60. Eser, B. E., and Fitzpatrick, P. F. Measurement of intrinsic rate constants in the tyrosine hydroxylase reaction, *Biochemistry 49*, 645-652.

61. Kumer, S. C., and Vrana, K. E. (1996) Intricate regulation of tyrosine hydroxylase activity and gene expression, *J Neurochem 67*, 443-462.

62. Campbell, D. G., Hardie, D. G., and Vulliet, P. R. (1986) Identification of four phosphorylation sites in the N-terminal region of tyrosine hydroxylase, *J Biol Chem 261*, 10489-10492.

63. Haycock, J. W. (1990) Phosphorylation of tyrosine hydroxylase in situ at serine 8, 19, 31, and 40, *J Biol Chem 265*, 11682-11691.

64. Sutherland, C., Alterio, J., Campbell, D. G., Le Bourdelles, B., Mallet, J., Haavik, J., and Cohen, P. (1993) Phosphorylation and activation of human

tyrosine hydroxylase in vitro by mitogen-activated protein (MAP) kinase and MAP-kinase-activated kinases 1 and 2, *Eur J Biochem 217*, 715-722.

65. Griffith, L. C., and Schulman, H. (1988) The multifunctional Ca2+/calmodulin-dependent protein kinase mediates Ca2+-dependent phosphorylation of tyrosine hydroxylase, *J Biol Chem 263*, 9542-9549.

66. Haycock, J. W., and Haycock, D. A. (1991) Tyrosine hydroxylase in rat brain dopaminergic nerve terminals. Multiple-site phosphorylation in vivo and in synaptosomes, *J Biol Chem 266*, 5650-5657.

67. Royo, M., Daubner, S. C., and Fitzpatrick, P. F. (2004) Specificity of the MAP kinase ERK2 for phosphorylation of tyrosine hydroxylase, *Arch Biochem Biophys 423*, 247-252.

68. Atkinson, J., Richtand, N., Schworer, C., Kuczenski, R., and Soderling, T. (1987) Phosphorylation of purified rat striatal tyrosine hydroxylase by Ca2+/calmodulin-dependent protein kinase II: effect of an activator protein, *J Neurochem 49*, 1241-1249.

69. Le Bourdelles, B., Horellou, P., Le Caer, J. P., Denefle, P., Latta, M., Haavik, J., Guibert, B., Mayaux, J. F., and Mallet, J. (1991) Phosphorylation of human recombinant tyrosine hydroxylase isoforms 1 and 2: an additional phosphorylated residue in isoform 2, generated through alternative splicing, *J Biol Chem 266*, 17124-17130.

70. Almas, B., Le Bourdelles, B., Flatmark, T., Mallet, J., and Haavik, J. (1992) Regulation of recombinant human tyrosine hydroxylase isozymes by

catecholamine binding and phosphorylation. Structure/activity studies and mechanistic implications, *Eur J Biochem 209*, 249-255.

71. Bevilaqua, L. R., Graham, M. E., Dunkley, P. R., von Nagy-Felsobuki, E. I., and Dickson, P. W. (2001) Phosphorylation of Ser(19) alters the conformation of tyrosine hydroxylase to increase the rate of phosphorylation of Ser(40), *J Biol Chem 276*, 40411-40416.

72. Toska, K., Kleppe, R., Armstrong, C. G., Morrice, N. A., Cohen, P., and Haavik, J. (2002) Regulation of tyrosine hydroxylase by stress-activated protein kinases, *J Neurochem 83*, 775-783.

73. Lehmann, I. T., Bobrovskaya, L., Gordon, S. L., Dunkley, P. R., and Dickson, P. W. (2006) Differential regulation of the human tyrosine hydroxylase isoforms via hierarchical phosphorylation, *J Biol Chem 281*, 17644-17651.

74. Moy, L. Y., and Tsai, L. H. (2004) Cyclin-dependent kinase 5 phosphorylates serine 31 of tyrosine hydroxylase and regulates its stability, *J Biol Chem 279*, 54487-54493.

75. Kleppe, R., Toska, K., and Haavik, J. (2001) Interaction of phosphorylated tyrosine hydroxylase with 14-3-3 proteins: evidence for a phosphoserine 40-dependent association, *J Neurochem 77*, 1097-1107.

76. Obsilova, V., Nedbalkova, E., Silhan, J., Boura, E., Herman, P., Vecer, J., Sulc, M., Teisinger, J., Dyda, F., and Obsil, T. (2008) The 14-3-3 protein affects the conformation of the regulatory domain of human tyrosine hydroxylase, *Biochemistry 47*, 1768-1777.

77. Daubner, S. C., Lauriano, C., Haycock, J. W., and Fitzpatrick, P. F. (1992) Site-directed mutagenesis of serine 40 of rat tyrosine hydroxylase. Effects of dopamine and cAMP-dependent phosphorylation on enzyme activity, *J Biol Chem 267*, 12639-12646.

78. Ramsey, A. J., and Fitzpatrick, P. F. (1998) Effects of phosphorylation of serine 40 of tyrosine hydroxylase on binding of catecholamines: evidence for a novel regulatory mechanism, *Biochemistry 37*, 8980-8986.

79. Ramsey, A. J., and Fitzpatrick, P. F. (2000) Effects of phosphorylation on binding of catecholamines to tyrosine hydroxylase: specificity and thermodynamics, *Biochemistry 39*, 773-778.

80. Ramsey, A. J., Hillas, P. J., and Fitzpatrick, P. F. (1996) Characterization of the active site iron in tyrosine hydroxylase. Redox states of the iron, *J Biol Chem 271*, 24395-24400.

81. Frantom, P. A., Seravalli, J., Ragsdale, S. W., and Fitzpatrick, P. F. (2006) Reduction and oxidation of the active site iron in tyrosine hydroxylase: kinetics and specificity, *Biochemistry 45*, 2372-2379.

82. Okuno, S., and Fujisawa, H. (1991) Conversion of tyrosine hydroxylase to stable and inactive form by the end products, *J Neurochem 57*, 53-60.

83. Lazar, M. A., Truscott, R. J., Raese, J. D., and Barchas, J. D. (1981) Thermal denaturation of native striatal tyrosine hydroxylase: increased thermolability of the phosphorylated form of the enzyme, *J Neurochem 36*, 677-682.

84. Vrana, K. E., Allhiser, C. L., and Roskoski, R., Jr. (1981) Tyrosine hydroxylase activation and inactivation by protein phosphorylation conditions, *J Neurochem 36*, 92-100.

85. Vrana, K. E., and Roskoski, R., Jr. (1983) Tyrosine hydroxylase inactivation following cAMP-dependent phosphorylation activation, *J Neurochem 40*, 1692-1700.

86. McCulloch, R. I., and Fitzpatrick, P. F. (1999) Limited proteolysis of tyrosine hydroxylase identifies residues 33-50 as conformationally sensitive to phosphorylation state and dopamine binding, *Arch Biochem Biophys 367*, 143-145.

87. Shiman, R., and Gray, D. W. (1980) Substrate activation of phenylalanine hydroxylase. A kinetic characterization, *J Biol Chem 255*, 4793-4800.

88. Abita, J. P., Milstien, S., Chang, N., and Kaufman, S. (1976) In vitro activation of rat liver phenylalanine hydroxylase by phosphorylation, *J Biol Chem 251*, 5310-5314.

89. Doskeland, A. P., Schworer, C. M., Doskeland, S. O., Chrisman, T. D., Soderling, T. R., Corbin, J. D., and Flatmark, T. (1984) Some aspects of the phosphorylation of phenylalanine 4-monooxygenase by a calcium-dependent and calmodulin-dependent protein kinase, *Eur J Biochem 145*, 31-37.

90. Kowlessur, D., Yang, X. J., and Kaufman, S. (1995) Further studies of the role of Ser-16 in the regulation of the activity of phenylalanine hydroxylase, *Proc Natl Acad Sci U S A 92*, 4743-4747.

91. Shiman, R., Mortimore, G. E., Schworer, C. M., and Gray, D. W. (1982) Regulation of phenylalanine hydroxylase activity by phenylalanine in vivo, in vitro, and in perfused rat liver, *J Biol Chem 257*, 11213-11216.

92. Doskeland, A. P., Martinez, A., Knappskog, P. M., and Flatmark, T. (1996) Phosphorylation of recombinant human phenylalanine hydroxylase: effect on catalytic activity, substrate activation and protection against non-specific cleavage of the fusion protein by restriction protease, *Biochem J 313 (Pt 2)*, 409-414.

93. Daubner, S. C., Hillas, P. J., and Fitzpatrick, P. F. (1997) Characterization of chimeric pterin-dependent hydroxylases: contributions of the regulatory domains of tyrosine and phenylalanine hydroxylase to substrate specificity, *Biochemistry 36*, 11574-11582.

94. Li, J., Dangott, L. J., and Fitzpatrick, P. F. (2010) Regulation of phenylalanine hydroxylase: conformational changes upon phenylalanine binding detected by hydrogen/deuterium exchange and mass spectrometry, *Biochemistry 49*, 3327-3335.

95. Okuno, S., and Fujisawa, H. (1982) Purification and some properties of tyrosine 3-monooxygenase from rat adrenal, *Eur J Biochem 122*, 49-55.

96. Nakata, H., and Fujisawa, H. (1982) Tryptophan 5-monooxygenase from mouse mastocytoma P815. A simple purification and general properties, *Eur J Biochem 124*, 595-601.

97. Haavik, J., Martinez, A., and Flatmark, T. (1990) pH-dependent release of catecholamines from tyrosine hydroxylase and the effect of phosphorylation of Ser-40, *FEBS Lett 262*, 363-365.

98. Goodwill, K. E., Sabatier, C., and Stevens, R. C. (1998) Crystal structure of tyrosine hydroxylase with bound cofactor analogue and iron at 2.3 A resolution: self-hydroxylation of Phe300 and the pterin-binding site, *Biochemistry 37*, 13437-13445.

99. Flockhart, D. A., and Corbin, J. D. (1984) Preparation of the Catalytic Subunit of Camp-Dependent Protein Kinase, in Brain Receptor Methodologies, Part A (Maranos, P. J., Campbell, I. C. and Cohen, R. M., Eds.) pp. 209-215. Academic Press, New York.

100. Weis, D. D., Engen, J. R., and Kass, I. J. (2006) Semi-automated data processing of hydrogen exchange mass spectra using HX-Express, *J Am Soc Mass Spectrom 17*, 1700-1703.

101. Zhang, Z., and Marshall, A. G. (1998) A universal algorithm for fast and automated charge state deconvolution of electrospray mass-to-charge ratio spectra, *J Am Soc Mass Spectrom 9*, 225-233.

102. McCulloch, R. I., and Fitzpatrick, P. F. (1999) Limited proteolysis of tyrosine hydroxylase identifies residues 33-50 as conformationally sensitive to phosphorylation state and dopamine binding, *Arch. Biochem. Biophys. 367*, 143-145.

103. Johnson, L. N., and O'Reilly, M. (1996) Control by phosphorylation, *Curr Opin Struct Biol 6*, 762-769.

104. Larkin, M. A., Blackshields, G., Brown, N. P., Chenna, R., McGettigan, P. A., McWilliam, H., Valentin, F., Wallace, I. M., Wilm, A., Lopez, R., Thompson, J. D., Gibson, T. J., and Higgins, D. G. (2007) Clustal W and Clustal X version 2.0, *Bioinformatics 23*, 2947-2948.

105. Bai, Y., Milne, J. S., Mayne, L., and Englander, S. W. (1993) Primary structure effects on peptide group hydrogen exchange, *Proteins 17*, 75-86.

106. Sura, G. R., Lasagna, M., Gawandi, V., Reinhart, G. D., and Fitzpatrick, P. F. (2006) Effects of ligands on the mobility of an active-site loop in tyrosine hydroxylase as monitored by fluorescence anisotropy, *Biochemistry 45*, 9632-9638.

107. Okuno, S., and Fujisawa, H. (1985) A new mechanism for regulation of tyrosine 3-monooxygenase by end product and cyclic AMP-dependent protein kinase, *J Biol Chem 260*, 2633-2635.

108. Wang, S., Sura, G. R., Dangott, L. J., and Fitzpatrick, P. F. (2009) Identification by hydrogen/deuterium exchange of structural changes in tyrosine hydroxylase associated with regulation, *Biochemistry 48*, 4972-4979.

109. Lakowicz, J. R. (1980) Fluorescence spectroscopic investigations of the dynamic properties of proteins, membranes and nucleic acids, *J Biochem Biophys Methods 2*, 91-119.

110. Gratton, E., Jameson, D. M., and Hall, R. D. (1984) Multifrequency phase and modulation fluorometry, *Annu Rev Biophys Bioeng 13*, 105-124.

111. Johnson, J. L., and Reinhart, G. D. (1994) Influence of MgADP on phosphofructokinase from Escherichia coli. Elucidation of coupling interactions with both substrates, *Biochemistry 33*, 2635-2643.

112. McCulloch, R. I., Daubner, S. C., and Fitzpatrick, P. F. (2001) Effects of substitution at serine 40 of tyrosine hydroxylase on catecholamine binding, *Biochemistry 40*, 7273-7278.

113. Alcala, J. R., Gratton, E., and Prendergast, F. G. (1987) Resolvability of fluorescence lifetime distributions using phase fluorometry, *Biophys J 51*, 587-596.

114. Alcala, J. R., Gratton, E., and Prendergast, F. G. (1987) Fluorescence lifetime distributions in proteins, *Biophys J 51*, 597-604.

115. Alcala, J. R., Gratton, E., and Prendergast, F. G. (1987) Interpretation of fluorescence decays in proteins using continuous lifetime distributions, *Biophys J 51*, 925-936.

116. Munro, I., Pecht, I., and Stryer, L. (1979) Subnanosecond motions of tryptophan residues in proteins, *Proc Natl Acad Sci U S A 76*, 56-60.

117. Lipari, G., and Szabo, A. (1980) Effect of librational motion on fluorescence depolarization and nuclear magnetic resonance relaxation in macromolecules and membranes, *Biophys J 30*, 489-506.

118. Halskau, O., Jr., Ying, M., Baumann, A., Kleppe, R., Rodriguez-Larrea, D., Almas, B., Haavik, J., and Martinez, A. (2009) Three-way interaction between 14-3-3 proteins, the N-terminal region of tyrosine hydroxylase, and negatively charged membranes, *J Biol Chem 284*, 32758-32769.

119. Bustos, D. M., and Iglesias, A. A. (2006) Intrinsic disorder is a key characteristic in partners that bind 14-3-3 proteins, *Proteins 63*, 35-42.

120. Erlandsen, H., Flatmark, T., Stevens, R. C., and Hough, E. (1998) Crystallographic analysis of the human phenylalanine hydroxylase catalytic domain with bound catechol inhibitors at 2.0 A resolution, *Biochemistry 37*, 15638-15646.

121. Hufton, S. E., Jennings, I. G., and Cotton, R. G. (1995) Structure and function of the aromatic amino acid hydroxylases, *Biochem J 311 (Pt 2)*, 353-366.

122. Ludecke, B., Knappskog, P. M., Clayton, P. T., Surtees, R. A., Clelland, J. D., Heales, S. J., Brand, M. P., Bartholome, K., and Flatmark, T. (1996) Recessively inherited L-DOPA-responsive parkinsonism in infancy caused by a point mutation (L205P) in the tyrosine hydroxylase gene, *Hum Mol Genet 5*, 1023-1028.

123. Kaufman, S. (1993) The phenylalanine hydroxylating system, *Adv Enzymol Relat Areas Mol Biol 67*, 77-264.

124. Nakata, H., and Fujisawa, H. (1982) Purification and properties of tryptophan 5-monooxygenase from rat brain-stem, *Eur J Biochem 122*, 41-47.

125. Doskeland, A., Ljones, T., Skotland, T., and Flatmark, T. (1982) Phenylalanine 4-monooxygenase from bovine and rat liver: some physical and chemical properties, *Neurochem Res 7*, 407-421.

126. Kappock, T. J., Harkins, P. C., Friedenberg, S., and Caradonna, J. P. (1995) Spectroscopic and kinetic properties of unphosphorylated rat hepatic phenylalanine hydroxylase expressed in Escherichia coli. Comparison of resting and activated states, *J Biol Chem 270*, 30532-30544.

127. Knappskog, P. M., Flatmark, T., Aarden, J. M., Haavik, J., and Martinez, A. (1996) Structure/function relationships in human phenylalanine hydroxylase. Effect of terminal deletions on the oligomerization, activation and cooperativity of substrate binding to the enzyme, *Eur J Biochem 242*, 813-821.

128. D'Sa, C. M., Arthur, R. E., Jr., and Kuhn, D. M. (1996) Expression and deletion mutagenesis of tryptophan hydroxylase fusion proteins: delineation of the enzyme catalytic core, *J Neurochem 67*, 917-926.

129. Fusetti, F., Erlandsen, H., Flatmark, T., and Stevens, R. C. (1998) Structure of tetrameric human phenylalanine hydroxylase and its implications for phenylketonuria, *J Biol Chem 273*, 16962-16967.

130. Liberles, J. S., Thorolfsson, M., and Martinez, A. (2005) Allosteric mechanisms in ACT domain containing enzymes involved in amino acid metabolism, *Amino Acids 28*, 1-12.

131. Grant, G. A. (2006) The ACT domain: a small molecule binding domain and its role as a common regulatory element, *J Biol Chem 281*, 33825-33829.

132. Jennings, I. G., Teh, T., and Kobe, B. (2001) Essential role of the N-terminal autoregulatory sequence in the regulation of phenylalanine hydroxylase, *FEBS Lett 488*, 196-200.

133. Wang, G. A., Gu, P., and Kaufman, S. (2001) Mutagenesis of the regulatory domain of phenylalanine hydroxylase, *Proc Natl Acad Sci U S A 98*, 1537-1542.

134. Thorolfsson, M., Teigen, K., and Martinez, A. (2003) Activation of phenylalanine hydroxylase: effect of substitutions at Arg68 and Cys237, *Biochemistry 42*, 3419-3428.

135. Martinez, A., Olafsdottir, S., and Flatmark, T. (1993) The cooperative binding of phenylalanine to phenylalanine 4-monooxygenase studied by 1H-NMR paramagnetic relaxation. Changes in water accessibility to the iron at the active site upon substrate binding, *Eur J Biochem 211*, 259-266.

136. Thorolfsson, M., Ibarra-Molero, B., Fojan, P., Petersen, S. B., Sanchez-Ruiz, J. M., and Martinez, A. (2002) L-phenylalanine binding and domain organization in human phenylalanine hydroxylase: a differential scanning calorimetry study, *Biochemistry 41*, 7573-7585.

137. Royo, M., Fitzpatrick, P. F., and Daubner, S. C. (2005) Mutation of regulatory serines of rat tyrosine hydroxylase to glutamate: effects on enzyme stability and activity, *Arch Biochem Biophys 434*, 266-274.

138. Krishna, M. M., Hoang, L., Lin, Y., and Englander, S. W. (2004) Hydrogen exchange methods to study protein folding, *Methods 34*, 51-64.

VITA

Shanzhi Wang

TAMU Dept of Biochemistry
103 Biochemistry Building
2128 TAMU
College Station, TX 77843-2128

shanzhi@tamu.edu

Education

B.S., Jilin University, 2004
Ph.D., Texas A&M University, 2010

Awards and Honors during Doctoral Studies

2009: travel grant award from Biochemistry Department of Texas A&M University.

Talks in Meetings

Texas Enzyme Mechanisms Conference, 01/2010, Austin, TX. Title: Identification of Structural Changes Associated with Regulation of Tyrosine Hydroxylase.

Publications

Wang, S., Sura, G. R., Dangott, L. J., and Fitzpatrick, P. F. (2009) Identification by hydrogen/deuterium exchange of structural changes in tyrosine hydroxylase associated with regulation. *Biochemistry 48*, 4972-4979.